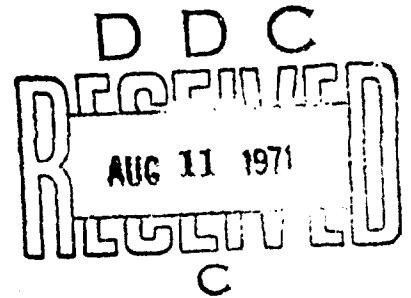AD728158

AD

Report 2005

EVALUATION OF NONEXPENDABLE MINE CLEARING

ROLLER WHEELS UNDER BLAST ATTACK

by

Bruce L. Morris

D D C

AUG 11 1971

April 1971

C

Approved for public release; distribution unlimited.

U. S. ARMY MOBILITY EQUIPMENT RESEARCH AND DEVELOPMENT CENTER
FORT BELVOIR, VIRGINIA

64

DOCUMENT CONTROL DATA - R & D

(Security classification of title, body of abstract and indexing annotation must be entered when the overall report is classified)

1. ORIGINATING ACTIVITY (Corporate author)	2a. REPORT SECURITY CLASSIFICATION
U. S. Army Mobility Equipment Research and Development Center	Unclassified
Fort Belvoir, Virginia	2b. GROUP NA

3. REPORT TITLE

EVALUATION OF NONEXPENDABLE MINE CLEARING ROLLER WHEELS UNDER BLAST ATTACK

4. DESCRIPTIVE NOTES (Type of report and inclusive dates)
Final Report, October 1970 to February 1971

5. AUTHOR(S) (First name, middle initial, last name)

Bruce L. Morris

6. REPORT DATE	7a. TOTAL NO. OF PAGES	7b. NO. OF REFS
April 1971	64	5

8a. CONTRACT OR GRANT NO.	9a. ORIGINATOR'S REPORT NUMBER(S)
b. PROJECT NO. 1J564606D415	2005
c. Task No. 1J564606D41511	9b. OTHER REPORT NO(S) (Any other numbers that may be assigned this report)
d.	

10. DISTRIBUTION STATEMENT

Approved for public release; distribution unlimited.

11. SUPPLEMENTARY NOTES	12. SPONSORING MILITARY ACTIVITY
Details of illustrations in this document may be better studied on microfiche	Army Materiel Command Washington, D. C. 20315

13. ABSTRACT

This project experimentally evaluated configurations and materials for mine clearing roller wheels required to withstand the effects of three detonations of 30 pounds of explosives each. The tests were conducted using one-fourth geometric scale-model wheels and suitably scaled explosive charges. 4340, T-1, HY-100, and 4330 steels were tested in a flat-rimmed and two curved-rim wheel configurations, and the impulse imparted to these wheels was experimentally determined.

The report concludes that:

a. The blast resistance of machined, curved-rim wheels (radius of rim curvature equals one-fourth of the wheel width) is approximately 25 percent better than that of flat-rimmed wheels of the same material (T-1 and 4340 steels).

b. Cast 4330, HY-100, and T-1 curved-rim wheels (radius of rim curvature equals two-fifths of the wheel width) provide a 138-percent blast-resistance increase over that of the machined T-1 flat-rimmed wheels; the 4330 is desirable because of its better chemical and mechanical properties and its lower production cost.

c. Cast steel appears to be a better candidate material than machined steel because of the former's non-laminar internal structure and its relative ease and low cost of quantity production.

d. Qualitative data generated by these tests indicate that the full-scale design may be practical and will satisfy the blast-resistance requirements.

e. Data generated on scaled specific impulse for scaled distances of 0.05 to 0.09 ft/lb$^{1/3}$ are seen to agree with extrapolated data obtained in the 4 to 50 scaled distance range.

Confirmatory tests will be conducted against full scale wheels, and the results will be presented in subsequent reports.

DD FORM **1473** REPLACES DD FORM 1473, 1 JAN 64, WHICH IS OBSOLETE FOR ARMY USE.

Destroy this report when no longer needed.
Do not return it to the originator.

— — — — — — — —

The citation in this report of trade names of commercially available products
does not constitute official endorsement or approval of the use of such products.

14. KEY WORDS	LINK A		LINK B		LINK C	
	ROLE	WT	ROLE	WT	ROLE	WT
near-field blast pressure						
near-field blast impulse						
buried explosives						
materials, steel						
blast resistance						
explosive cratering						

1   3-4   32 934 - Ft Belvoir

U. S. ARMY MOBILITY EQUIPMENT
RESEARCH AND DEVELOPMENT CENTER
FORT BELVOIR, VIRGINIA

Report 2005

EVALUATION OF NONEXPENDABLE MINE CLEARING

ROLLER WHEELS UNDER BLAST ATTACK

Project 1J564606D41511

April 1971

Distributed by

The Commanding Officer
U. S. Army Mobility Equipment Research and Development Center

Prepared by

Bruce L. Morris
Mine Neutralization Division
Military Technology Laboratory

SUMMARY

This project experimentally evaluated configurations and materials for mine clearing roller wheels required to withstand the effects of three detonations of 30 pounds of explosives each. The tests were conducted using one-fourth geometric scale-model wheels and suitably scaled explosive charges. 4340, T-1, HY-100, and 4330 steels were tested in a flat-rimmed and two curved-rim wheel configurations, and the impulse imparted to these wheels was experimentally determined.

The report concludes that:

a.   The blast resistance of machined, curved-rim wheels (radius of rim curvature equals one-fourth of the wheel width) is approximately 25 percent better than that of flat-rimmed wheels of the same material (T-1 and 4340 steels).

b.   Cast 4330, HY-100, and T-1 curved-rim wheels (radius of rim curvature equals two-fifths of the wheel width) provide a 138-percent blast-resistance increase over that of the machined T-1 flat-rimmed wheels; the 4330 is desirable because of its better chemical and mechanical properties and its lower production cost.

c.   Cast steel appears to be a better candidate material than machined steel because of the former's nonlaminar internal structure and   relative ease and low cost of quantity production.

d.   Qualitative data generated by these tests indicate that the full-scale design may be practical and will satisfy the blast-resistance requirements.

e.   Data generated on scaled specific impulse for scaled distances of 0.05 to 0.09 ft/lb$^{1/3}$ are seen to agree with extrapolated data obtained in the 4 to 50 scaled distance range.

Confirmatory tests will be conducted against full scale wheels, and the results will be presented in subsequent reports.

FOREWORD

This investigation was conducted under the authority of U. S. Army Materiel Command Project 1J564606D41511, "Nonexpendable Mine Clearing Roller."

The tests were performed at the Barrier Experimental Facility, U. S. Army Mobility Equipment Research and Development Center annex, from October 1970 to January 1971.

The investigation was under the direct supervision of Bruce L. Morris, Mine Neutralization Division, Military Technology Laboratory. Field support was provided by personnel of the Barrier Experimental Facility, and pictorial support was provided by the RD. ' Pictorial Support Division.

CONTENTS

ILLUSTRATIONS

v

TABLES

EVALUATION OF NONEXPENDABLE MINE CLEARING

ROLLER WHEELS UNDER BLAST ATTACK

I. INTRODUCTION

1. **Subject.** This report covers the procedures and results of scale-model tests conducted to evaluate designs and materials for nonexpendable mine clearing roller wheels required to withstand the effects of three detonations of 30 pounds of explosives each. Tests were conducted by detonating small blocks of composition C-4 explosive (0.106 to 0.661 pounds) against a test rig holding either one or three test wheels. Data permitting calculation of the energy and impulse imparted to the test wheel(s) were recorded, and the ability of the wheel to withstand the blast effects was qualitatively evaluated.

The results of this test will be utilized in the final selection of design configuration and material for nonexpendable mine clearing roller wheels and will provide data in the area of near-field blast effects.

2. **Background.** The advent of mine warfare in World War I prompted the need for a device capable of clearing land mines and withstanding the effects of the resulting blasts. With World War II came the emphasis on mine clearing rollers—devices consisting of sets of wheels or discs pushed in front of a vehicle to detonate land mines. All such devices designed between 1942 and 1960 were either so heavy as to be unmaneuverable or were not capable of withstanding the blast effects of standard antitank mines.[1]

The 1960's saw the advent of the expendable mine clearing rollers: devices designed so that a quickly replaceable portion of the roller is destroyed, or expended, with each mine encounter. Developments in this area showed that portions of the roller not in the immediate vicinity of the blast (i.e., all portions other than the wheels and connecting yokes) are undamaged by blast effects and can thus be fabricated of nonexotic materials without excessive weight.

The main technical objective in the development of a nonexpendable mine clearing roller is thus the design of a lightweight wheel capable of withstanding the resulting blast effects. These effects include the blast pressure itself and the resulting impulse imparted to the wheel. A major portion of the impulse is provided by the soil

---

[1] U.S. Army Mobility Equipment Research and Development Center, "Historical Excerpts of Mine Warf : Research and Development, 1942-1959," Technical Report 1924, Fort Belvoir, Virginia, March 1968.

being thrown out of the crater resulting from the blast. The rapid heating caused by the blast provides another loading on a near-field target.

With maximum impact resistance as the primary criterion, the Metallurgy Section, under the direction of Mr. W. H. Baer, of the U. S. Army Mobility Equipment Research and Development Center (USAMERDC) Materials Research Support Division conducted a review of available materials and recommended the following steels as suitable for use in mine clearing roller wheels:

| AISI | 4330, Class 10Q (Low-alloy steel castings suitable for pressure service). |

| ASTM | A487, Class 7Q (T-1) (Low-alloy steel castings suitable for pressure service). |

| HY-100 | Mil-S-23008 (Steel castings, alloy, high yield strength). |

| HY-100 | Mil-S-23009 (Steel forgings, alloy, high yield strength). |

Tests to determine the optimum width, diameter, and spacing to provide optimum load transfer for mine clearing roller wheels were conducted by USAMERDC. These tests concluded that, of the wheel configurations tested, 22-inch-diameter, 3-inch-wide wheels spaced 8 inches, center-to-center, produced the desired load transfer for the least total weight for an operational roller. A report of these tests is given in Appendix A.

Southwest Research Institute, prime contractor on Contract DAAK02-70-C-0579, Design, Development and Delivery of Components for Nonexpendable Mine Clearing Roller, developed a computer program to predict ground stresses under mine clearing roller wheels. The results of this program are substantially the same as the USAMERDC tests, but it was felt that a wider wheel would be necessary to withstand the side loadings from mine detonations under adjacent wheels. Combining performance in the load transfer test and expected blast resistance, 28-inch-diameter, 4-inch-wide wheels spaced at 7.5 inches, center-to-center, were selected.

II. INVESTIGATION

3. **Scaling Laws.** The blast tests were conducted using one-fourth geometric scale models of the prototype roller wheels. In order to correctly interpret the results of the experiment, it was necessary to determine the Pi terms governing the phenomena. A set of physical parameters that should govern blast waves in air and soil are given in Table I with their dimensions in a force-length-time (FLT) system.

2

Table 1. Physical Parameters Governing Explosive Effects

Symbol	Description	Units
P	Blast pressure	FL^{-2}
t	Time	T
ρ	Mass density of soil	$FL^{-4} T^2$
c	Seismic velocity of soil	LT^{-1}
L	Characteristic length	L
r_i	Shape of system	---
M	Mass of wheel	$FL^{-1} T^{-2}$
g	Acceleration of gravity	LT^{-2}
f	Total load on wheel	F
E	Energy absorbed in wheel system	FL
a	Acceleration of wheel under blast	LT^{-2}
l	Impulse applied to wheel	$FL^{-2} T$
σ	Stress in wheel	FL^{-2}

        Ten dimensionless products can be formed from these 13 parameters (see details in Appendix B) and are presented below:

$$\pi_1 = \frac{t\,L^{\frac{1}{2}}\,P^{\frac{1}{2}}}{M^{\frac{1}{2}}}$$

$$\pi_2 = \frac{\rho\,L^3}{M\,P}$$

$$\pi_3 = \frac{c\,M^{\frac{1}{2}}}{L^{3/2}\,P^{1/2}}$$

Time scaling soil conditions

3

$$\pi_4 = r_i$$

$$\pi_5 = \frac{gM}{L^2 P}$$

$$\pi_6 = \frac{f}{P L^2}$$

⎫
⎬   Initial conditions and restraints
⎭

$$\pi_7 = \frac{E}{P L^3}$$

$$\pi_8 = \frac{aM}{P L^2}$$

$$\pi_9 = \frac{I L^{\frac{1}{2}}}{P^{\frac{1}{4}} M^{\frac{1}{4}}}$$

$$\pi_{10} = \frac{\sigma}{P}$$

⎫
⎬   Response scaling
⎭

For scale models, $\dfrac{L_m}{L_p} = \lambda, \lambda < 1$, where m and p denote model and prototype, respectively. If the same material is used in the model and prototype wheels, $\dfrac{M_m}{M_p} = \lambda^3$. We assume equality of blast pressures, i.e., $P_m = P_p$. These ratios are applied to the Pi terms to establish the scaling laws as shown below:

Scaling Law	Interpretation
$\pi_1 - t_m = \lambda\, t_p$	Time scales as the length ratio.
$\pi_2 - \rho_m = \rho_p$ $\pi_3 - c_m = c_p$	Same soil for model and prototype.
$\pi_4 - (r_i)_m = (r_i)_p$	Geometric similarity.
$\pi_5 - g_m = \dfrac{1}{\lambda}\, g_p$	Since the model and prototype tests are conducted in the same gravitational field, this term is distorted as an engineering judgment.

4

$\pi_6 - fm = \lambda^2 f_p$ Loads scale as the square of the length ratio to provide equal stresses.

$\pi_7 - Em = \lambda^3 E_p$ Energy scales as the cube of the length ratio, as does the charge weight.

$\pi_8 - am = \frac{1}{\lambda} a_p$ Acceleration scales as inverse time.

$\pi_9 - lm = \lambda l_p$

$\pi_{10} - \sigma m = \sigma_p$

Blast pressure is a function of the charge weight W and standoff distance R as $P = f(R/W^{1/3})$. Thus, if $Rm = \lambda R_p$, $Wm = \lambda^3 W_p$.

4. Test Equipment. A 3.5- by 2.5- by 2.5-foot soil-filled box (Fig. 1) was fabricated to serve as a rigid support for the test fixture. Three 1-inch-thick, rubber, torsion-spring sections (rotational modulus of 393 pounds per inch per degree for each section) to support the test wheels and yokes were mounted to the test box. One or three test wheels were placed in the three yokes using a common axle to help absorb sideloading on the yokes. All wheels had a 1/8-inch-thick nylon bushing separating them from the common axle. The yokes were secured to the torsion springs by four common pins, and scribes (as seen in Fig. 1) were used to measure the maximum rotation of the springs under the blast loading. Attempts to measure the wheel acceleration, using Endevco accelerometers, failed to produce any data.

5. Test Procedure. Test explosive charges were cut from demolition block M5A1; the 2- by 2- by 11-inch, 2.5-pound block of composition C-4 explosive was cut to the length necessary to provide the desired charge weight. The charges were detonated using M-6 blasting caps placed in the charge, such that the 2- by 2-inch face was nearest the target wheels.

The explosive charge was placed under the test wheels, so that the charge was directly under the center wheel with the blasting cap pointing toward the test box, as shown in Fig. 2. A 1/2-inch soil cover was placed over the charge, and the test wheels were lowered until they rested on the ground. The charge depth was such that a slight preload existed on the springs to simulate the total load on an operational roller wheel.

Wheels of different materials and configurations were placed in the test yokes and were subjected to detonations of increasing amounts of explosives. Initial cracking

5

RUBBER TORSION SPRING

TEST YOKE

SCRIBE

NOT REPRODUCIBLE
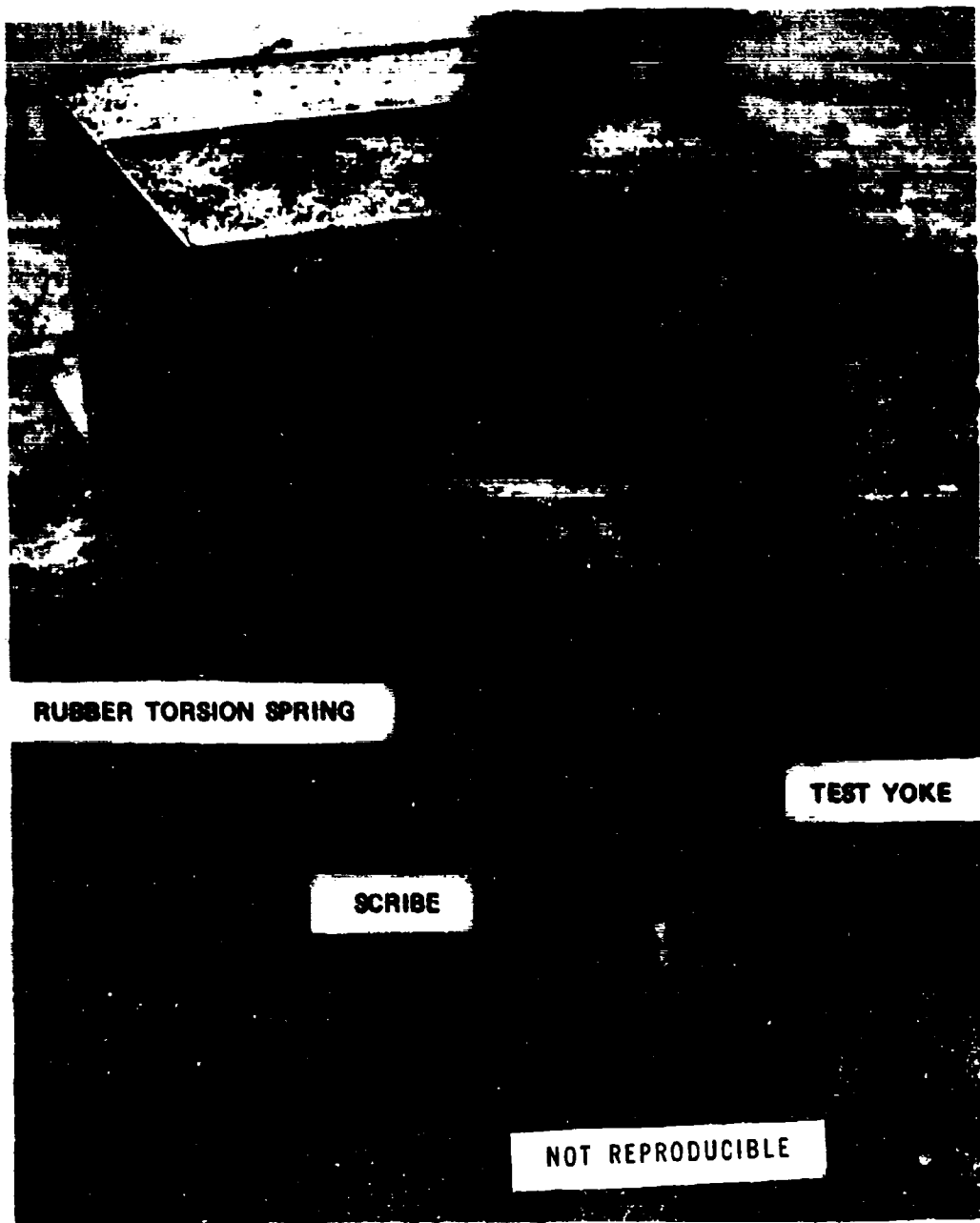
T2626

Fig. 1. Test box showing rubber torsion springs, scribes, and test yokes.

6

T2628

NOT REPRODUCIBLE

Fig. 2. Placement of explosive charge under test wheels.

was used as failure criteria. Data items recorded included charge weight, wheel material and configuration, number of wheels in test yokes, spring rotation (where possible), crater size, and qualitative ability of the wheel to withstand the blast effects.

Confirmatory tests will be conducted against full scale wheels, and the results will be presented in subsequent reports.

III. DISCUSSION

6. **Blast Resistance of Flat-Rimmed Machined Wheels.** Three wheels each of T-1 and 4340 steels (4340 selected for machining over 4330 because of in-house availability) were machined from rolled stock, as in Fig. 3. The mechanical properties of the as-tested wheels are given in Table II.

Table II. As-Tested Properties of T-1 and 4340 Machined Wheels (Flat-Rimmed)

Property	T-1	4340
Yield strength	103,000 psi	115,000 psi
Tensile strength	118,000 psi	122,000 psi
Elongation (in 2 inches)	12.5 percent	5.8 percent
Hardness	24 Rockwell "C"	26.5 Rockwell "C"

Thre three-wheel setup was used to test the T-1 wheels at equivalent charges of 7.5, 14.7, and 18.2 pounds (shots 1 to 3, respectively). The wheels were rotated approximately 90° after each shot. The two lower charges produced abrasion of the wheel surfaces facing the blast and relatively minor plastic flattening of the center-wheel rim with no appearance of cracking. The 18.2-pound shot produced cracking and spalling on the center wheel, as shown in Figs. 4 through 6 and described below. A spalled section 2.05 inches wide by 0.236 inch deep was removed from the wheel rim directly over the charge (Figs. 4 and 5). For these three shots, the charge was placed with the blasting cap pointing parallel to the test box. In this position, the blast wave was propagated at the side of the center wheel. This initial compressive wave was reflected as a tensile wave off the face shown in Fig. 4, causing the spall. The 2.05-inch spall width compares to the 2-inch charge width. The direction of propagation is also shown by the abrasion pattern in Fig. 5. The rim over the charge was pushed outward, and the inside of the rim cracked through, as shown in Figs. 4 and 6.
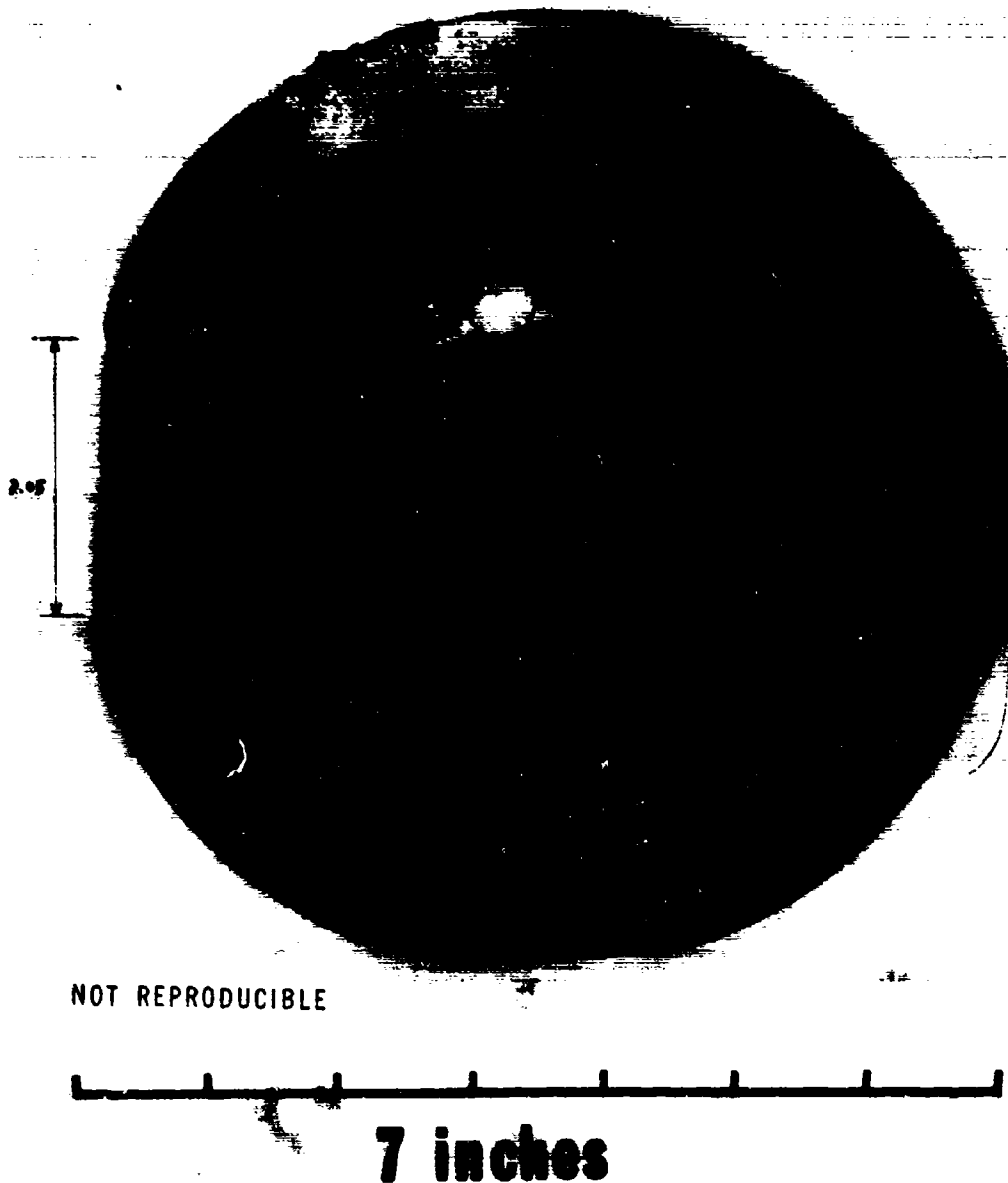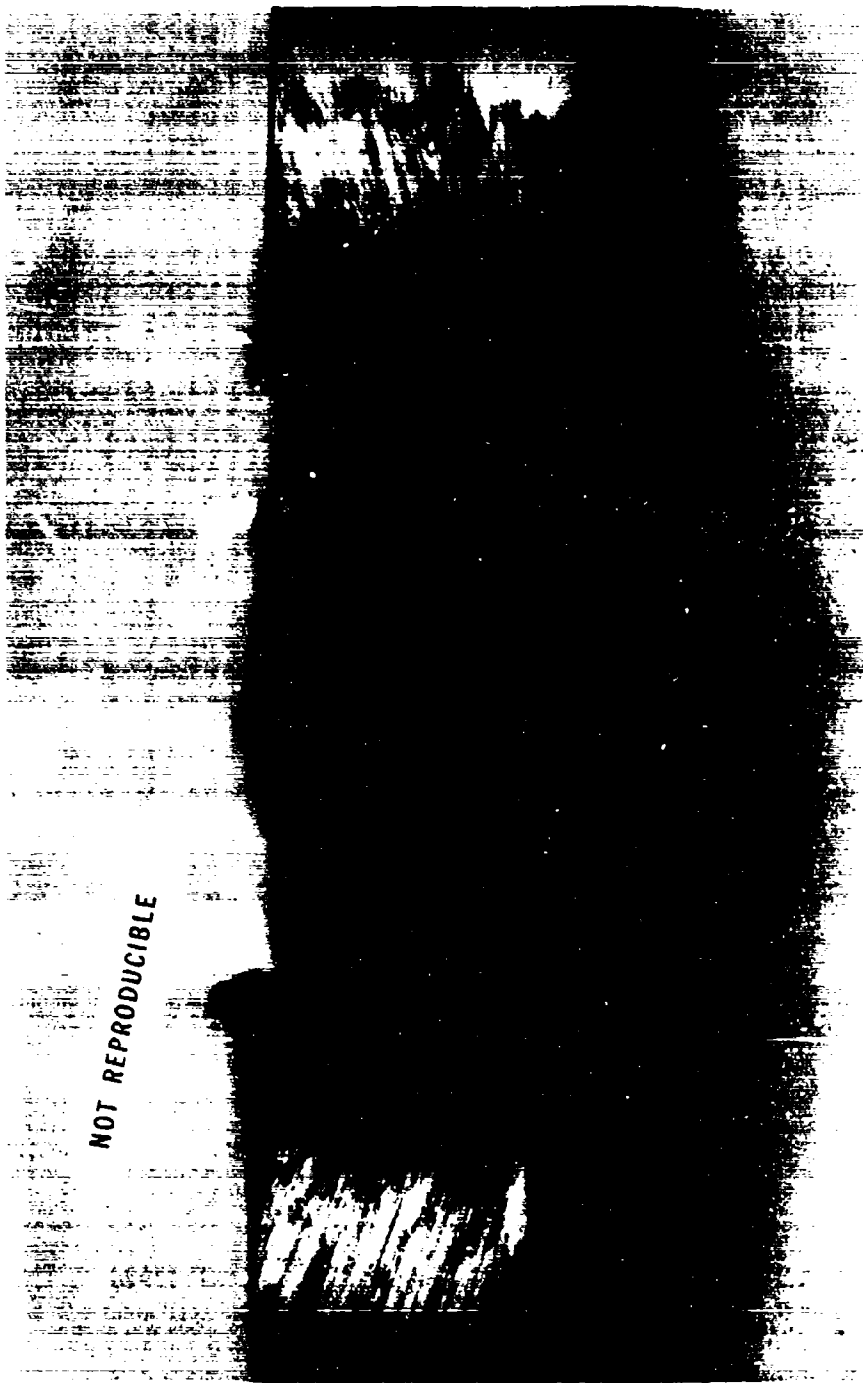
8

NOTE: ALL DIMENSIONS IN INCHES
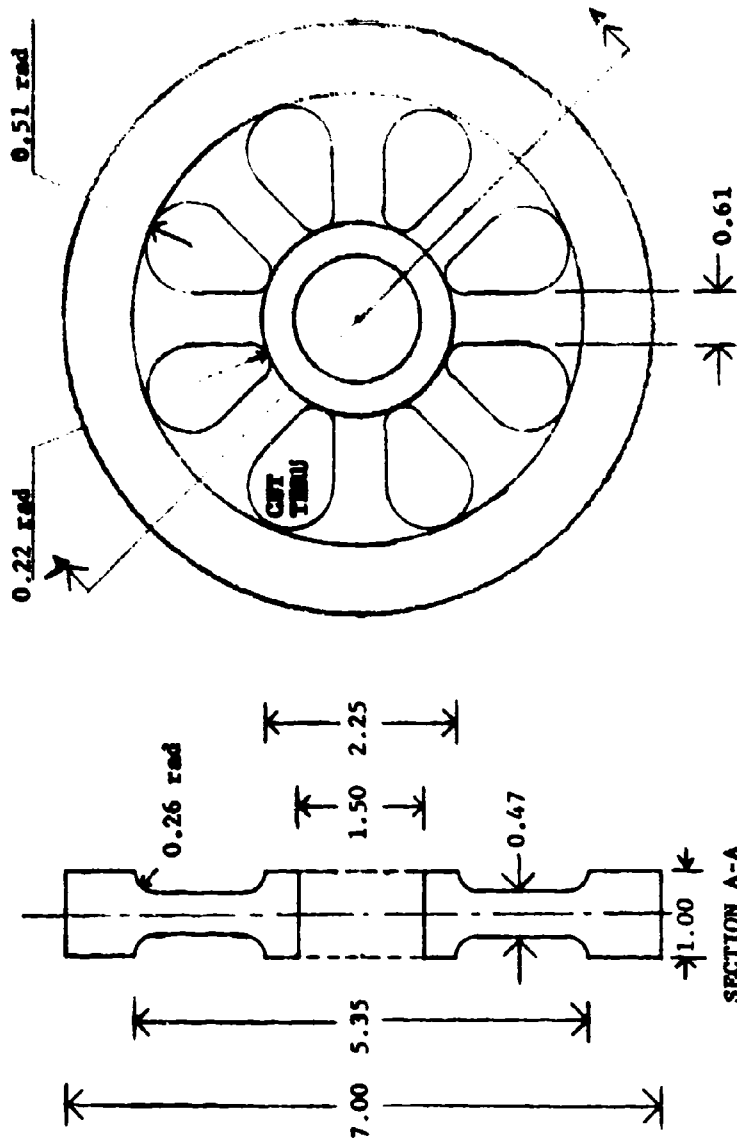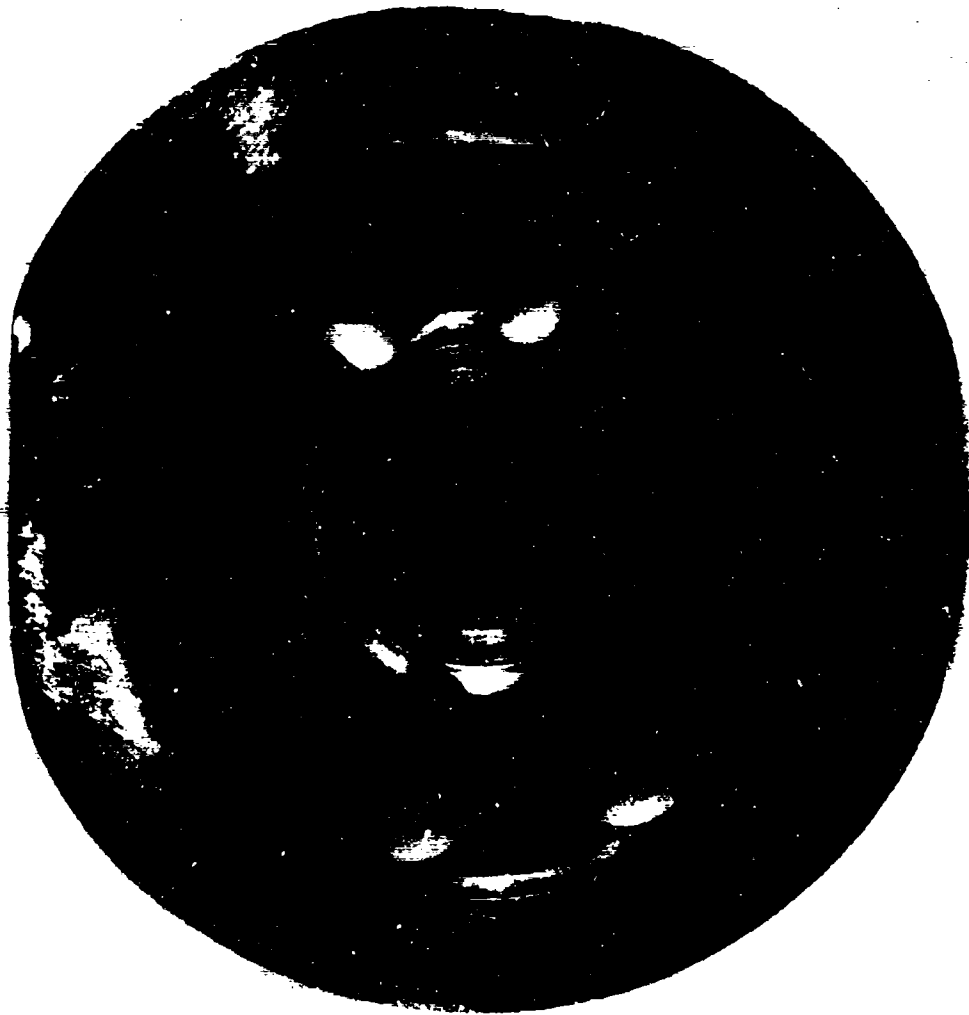
Fig. 3. Design of flat-rimmed wheel (machined).

9

2.05

7 inches

T3997

Fig. 4. T-1, flat-rimmed wheel showing spall area.

Fig. 5. Rim view of T-1, flat-rimmed wheel showing spall area and surface abrasion.

T3994

11

NOT REPRODUCIBLE

7 inches

T3996

Fig. 6. T-1, flat-rimmed wheel showing rim crack behind spall area.

The 4340 wheels, in the three-wheel setup, were subjected to blasts equivalent to 6.8, 12.8, and 13.2 pounds (shots 4 to 6, respectively). The wheels were rotated approximately 90° after each shot. These shots served to decrease the rim thickness over the blasts from 0.92 inch to 0.78 inch, increase the rim width from 1 inch to 1.28 inches, and misshape the center wheel. No apparent damage was caused to the side wheels, and no cracks appeared in the center wheel.

The left and center 4340 wheels were interchanged and subjected to blasts equivalent to 21.8 and 26.8 pounds (shots 7 and 8, respectively). The second shot cracked two bottom spokes in the left wheel, which had previously withstood the 6.8-, 12.8-, and 18.2-pound shots.

A 4340 flat-rimmed wheel, apparently undamaged by shots 4 to 8, was placed alone in the test rig. This single wheel was subjected to shots equivalent to 18.2, 21.8, 25.2, and 27.4 pounds (shots 14 to 17, respectively). The wheel was rotated approximately 60° after each shot. Shots 14 and 15 flattened the rim somewhat, and shot 16 cracked one spoke at the hub 90° from the charge axis (between shots 14 and 15). The wheel was still operable. Shot 17 cracked through one additional spoke and partially cracked two others. Three of these cracks can be seen in Fig. 7.

7. **Blast Resistance of Curved-Rim Machined Wheels.** One undamaged T-1 wheel was modified and three 4340 wheels were machined from round stock, as in Fig. 8. The mechanical properties of the T-1 wheel are as in Table II, and those of the 4340 wheels are given in Table III.

Table III. As-Tested Properties of 4340 Machined Wheels (Curved Rim)

Property	4340
Yield strength	107,158 psi
Tensile strength	115,677 psi
Elongation	7.1 percent

The T-1 wheel was tested in the three-wheel configuration using flat-rimmed wheels for the side wheels. This setup was subjected to blasts equivalent to 18.2 and 24.3 pounds (shots 9 and 10, respectively). Shot 9 caused no cracking and only slight abrasion of the center wheel rim. Shot 10 caused a crack on the inside of the rim immediately over the blast. This crack is shown in Figs. 9 and 10. The rim width over the charge was increased by the blast from 1 to 1.13 inches, and the wheel diameter
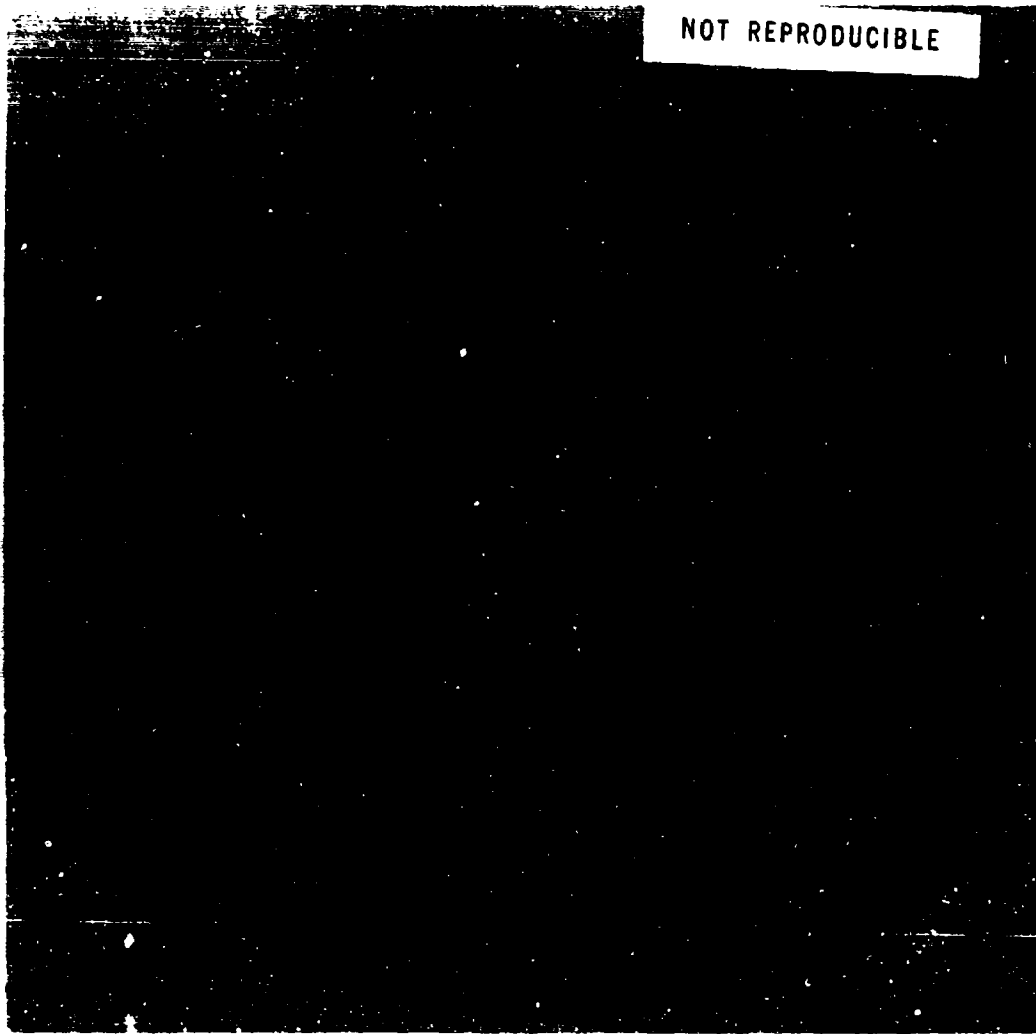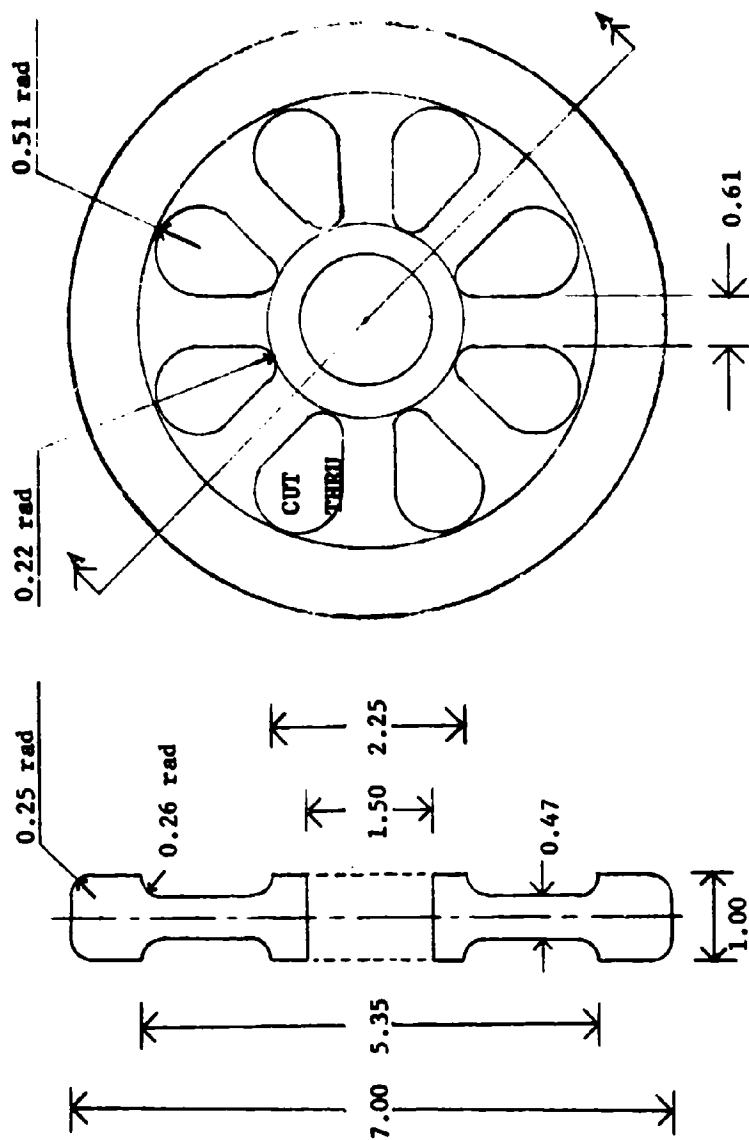
13

NOT REPRODUCIBLE

T2633

Fig. 7. Spoke cracks in 4340 flat-rimmed wheel.

14

NOTE: ALL DIMENSIONS IN INCHES

Fig. 8. Design of curved-rim wheel (machined).

15

NOT REPRODUCIBLE

T2637

Fig. 9. T-1 curved-rim wheel (machined) showing rim deformation and crack.

16

T2638

Fig. 10. Rim crack in T-1 curved-rim wheel (machined).

17

was decreased proportionally. The 4340 wheels were tested in the three-wheel configuration and were subjected to blasts equivalent to 26.8, 30, and 30 pounds (shots 11 to 13, respectively). The wheels were rotated 90° after each shot. Shots 11 and 12 served only to flatten the rim of the center wheel. Shot 13 cracked five spokes through at the hub of the left wheel and displaced the bottom of this wheel 1/4 inch outward with respect to the top of the wheel. This shear failure (showing the laminated character of the rolled material) is shown in Fig. 11. The center wheel rim cracked through at the point of blast and 180° from the blast (place of shot 11). The hub cracked through at three places, and two spokes cracked through, leaving the wheel in two pieces. This damage is shown in Fig. 12. A sectional view of the cracks, again showing the laminated material structure, is shown in Fig. 13.

Even though these 4340 wheels were fabricated according to the same drawing as the flat-rimmed wheels (except for the rim rounding), the cutout regions in the web of the curved-rim wheels extend farther into the web and the hub. The spokes in the curved wheels are narrower, and the cutouts extend approximately 1/8 inch farther into the hub and rim. This difference can be observed by comparing Figs. 4 and 11.

8. **Blast Resistance of Curved-Rim Cast Wheels.** Three wheels each of 4330, HY-100, and T-1 steel were cast according to Fig. 14, and were designated heats 1 through 3, respectively. Visual examination showed that one of the 4330 wheels failed to meet the class 2 (ASTM-E71) radiographic requirements, and two additional wheels were cast as heat 1a. Later examination showed that two each of the HY-100 and T-1 wheels did not meet the class 2 radiographic requirements, but they were not recast. The chemical and mechanical properties, as specified and as cast, for these wheels are given in Table IV. Complete casting data, including heat treatment used, are given in Appendix C.

The 4330 wheels were tested in the three-wheel configuration with a heat 1 wheel in the center position and heat 1a wheels on the sides. The wheels were subjected to blasts equivalent to 24.3, 26.8, 30 (three blasts), and 35 pounds (shots 18 to 23, respectively). The wheels were rotated approximately 90° after each shot. Shots 18 to 22 caused only abrasion and rim flattening less than that observed in previous shots. After shot 23, the minimum wheel diameter was 6.8 inches, the minimum rim thickness was 0.9 inch, and the bottom rim was 0.25 inch closer to the hub than the top rim. The wheel had not cracked and was still partially operable.

A single heat 1 4330 wheel was subjected to blasts equivalent to 30, 38.8, and 42.3 pounds (shots 24, 25, and 32, respectively). The wheel was rotated 90° between shots 24 and 25. The first two shots caused minor plastic deformation similar to, but not as excessive as, that previously observed. The wheel was still operable at this point. Shot 32 deformed the wheel, so that it was no longer operable and initiated

18

Table IV. Properties of Cast Wheels

	Heat 1 4330	Heat 1a 4330	Specification ASTM, A487, Class 10Q	Heat 2 HY-100	Specification MIL-S-23008	Heat 3 T-1	Specification ASTM, A487, Class 7Q
Chemical Composition							
Carbon	0.27%	0.27%	0.30% max	0.21%	0.22% max	0.17%	0.20% max
Manganese	0.71%	0.94%	0.60–1.00%	0.68%	0.55–0.75%	0.81%	0.60–1.00%
Chromium	0.63%	0.78%	0.55–0.90%	1.49%	1.35–1.85%	0.55%	0.40–0.80%
Nickel	1.75%	1.80%	1.40–2.00%	3.15%	2.75–3.50%	0.83%	0.70–1.00%
Molybdenum	0.30%	0.35%	0.20–0.40%	0.49%	0.30–0.60%	0.58%	0.40–0.60%
Copper	0.03%	0.04%	0.50% max	0.02%	–	0.33%	0.15–0.50%
Sulfur	0.02%	0.02%	0.045% max	0.017%	–	0.03%	–
Vanadium	–	–	–	–	–	0.07%	0.03–0.10%
Boron	–	–	–	–	–	0.009%	0.002–0.006%
Mechanical Properties							
Tensile strength	128,094 psi	129,797 psi	125,000 psi min	121,500 psi	100–200 Ksi	151,900 psi	115,000 psi min
Yield strength	113,285 psi	110,833 psi	100,000 psi min	102,600 psi		139,700 psi	100,000 psi min
Elongation (in 2″)	18.2%	18.0%	15% min	16%	18% min	11%	15% min
Reduction of area	–	–	35% min	–	30% min	–	30% min
Impact-Charpy V	27 ft-lb @ 72°	42 ft-lb @ 72°	15 ft-lb @ -50°	–	30 ft-lb @ -100°	–	15 ft-lb @ -50°
Hardness	27.5 Rc	–	–	26 Rc	–	34 Rc	–

19
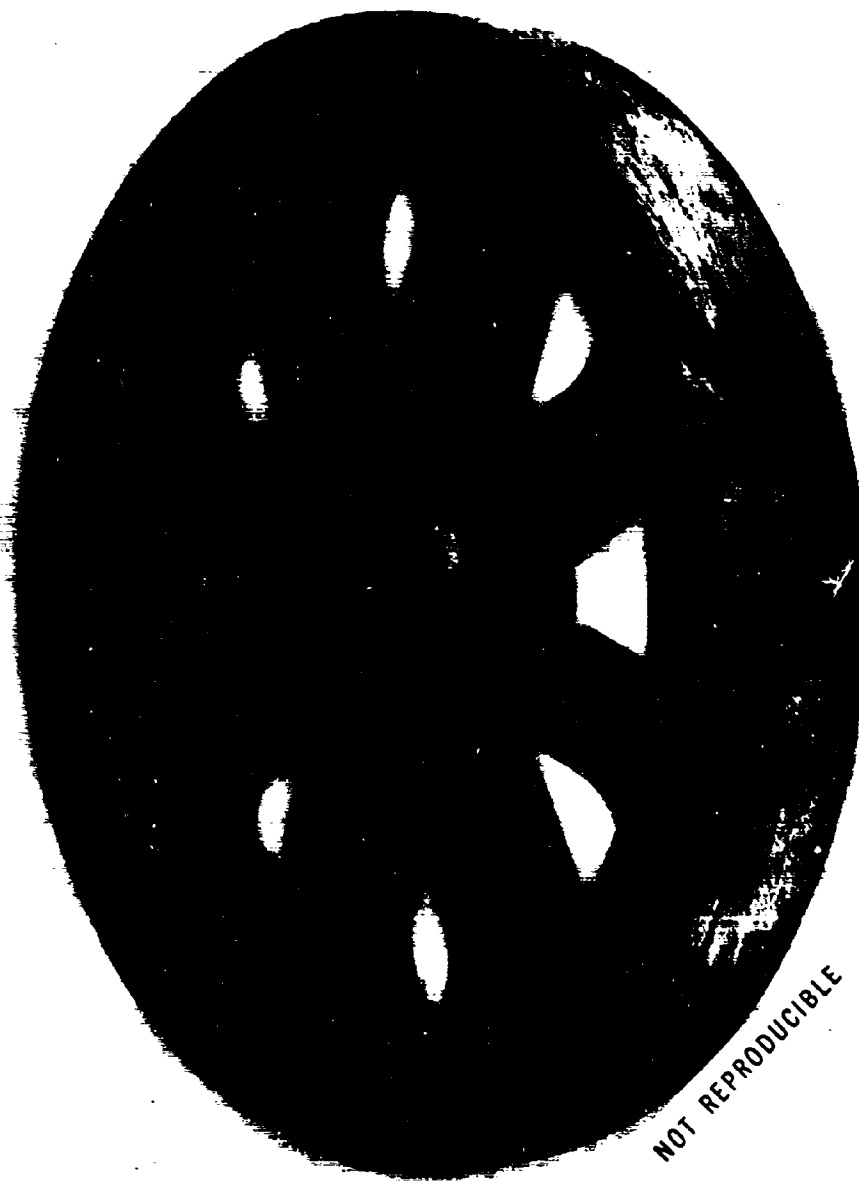
Fig. 11. Spoke cracks in 4340 curved-rim wheel (machined).

T4436

20
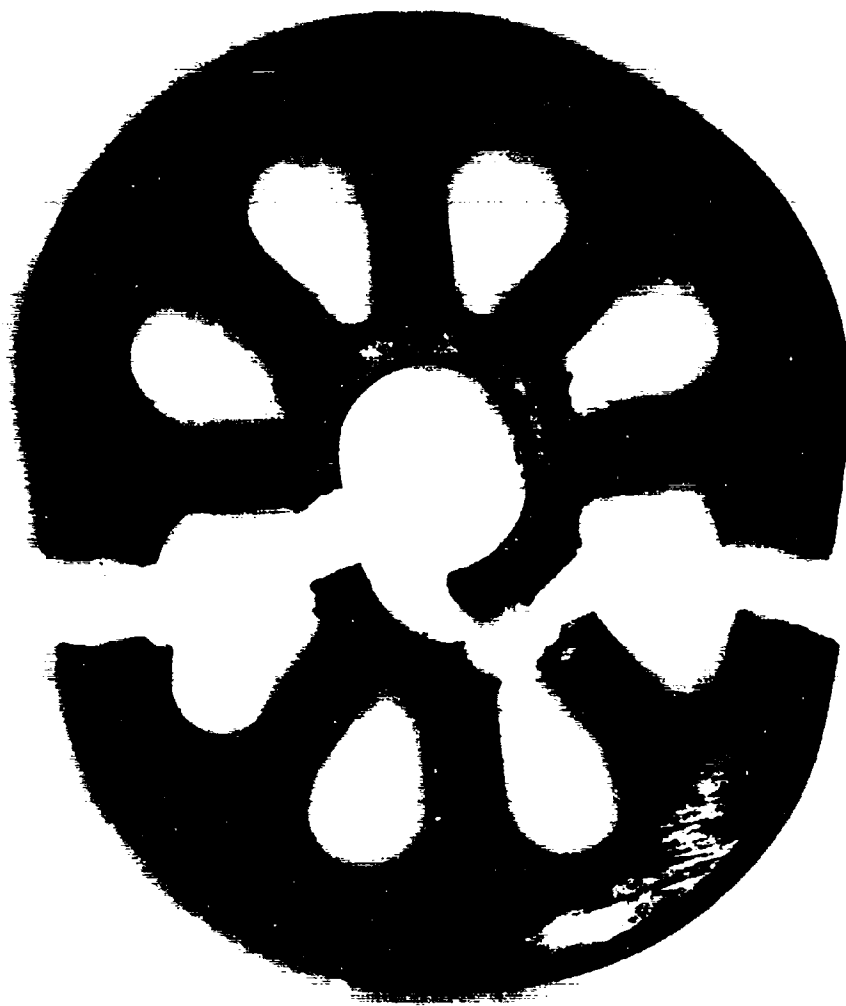
NOT REPRODUCIBLE

T4438

Fig. 12. 4340 curved-rim wheel (machined).

21

NOT REPRODUCIBLE

T4435

Fig. 13. Sectional view of 4340 curved-rim wheel (machined).

22

0.49 rad

0.61

0.22 rad

0.40 rad

0.12 rad

2.25

1.50

0.12 rad

0.47

1.00

5.10

7.00

SECTION A-A

NOTE: ALL DIMENSIONS IN INCHES

Fig. 14. Cast wheel design.

23

a crack on the inside of the rim directly over the blast. This damage can be seen in Figs. 15 and 16.

The sound T-1 cast wheel was tested in the center position of the three-wheel configuration with the unsound T-1 wheels on the sides. The wheel was subjected to blasts equivalent to 30, 35, and 39.5 pounds (shots 26 to 28, respectively). The wheels were rotated approximately 90° after each shot. The first two shots caused no operational damage to any wheel and only flattened the center rim. Shot 28 displa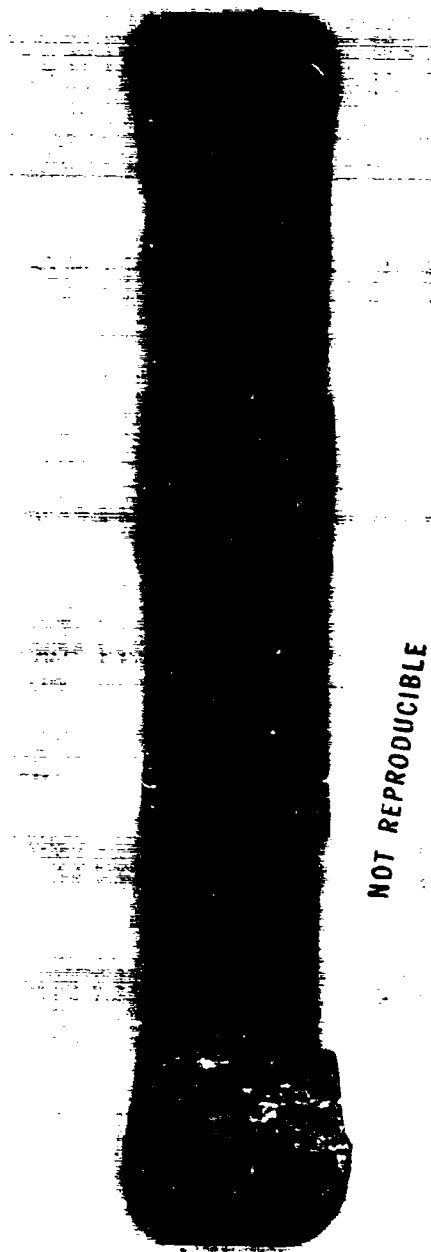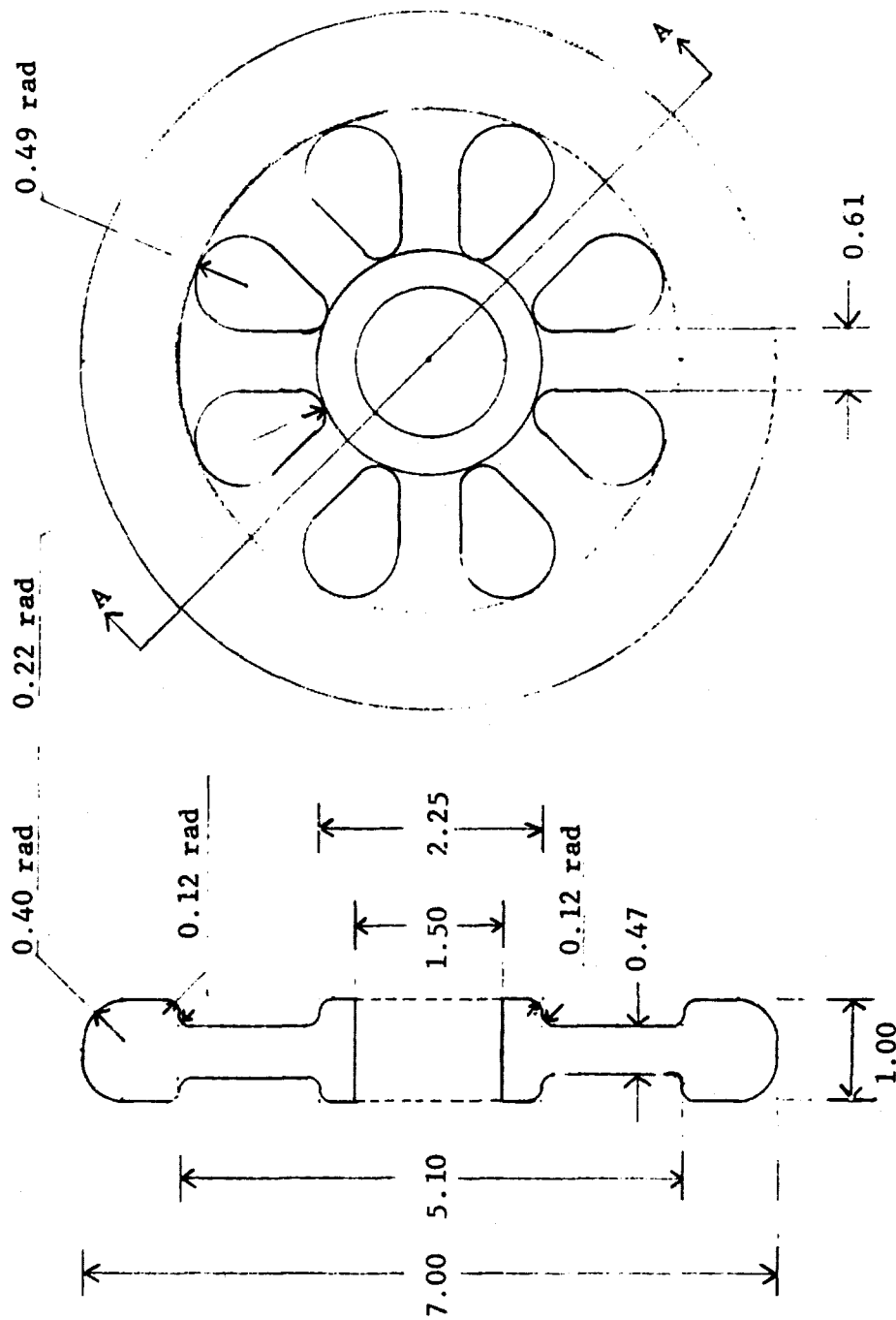ced the bottom of the right wheel approximately 3/8 inch, with respect to the top of the wheel, without cracking any spokes. The left wheel was bent outward slightly. The center wheel began to spall on the inside of the rim directly over the blast. This spalling was not sufficient to render the wheel inoperable. The damage can be seen in Figs. 17 and 18.

The acceptable HY-100 cast wheel was placed in the single-wheel configuration and was subjected to blasts equivalent to 30, 35, and 39.5 pounds (shots 29 to 31, respectively). Shot 29 flattened the rim more than was observed for the T-1 cast wheel. Shot 30 caused no damage other than additional rim flattening. Shot 31 caused no cracking, but deformed the wheel sufficiently to make it inoperable. This cumulative damage is shown in Fig. 19.

9. **Energy and Impulse Measurements.** The scribes, shown in Fig. 1, were used to measure the spring rotation under the blast loading. They worked reliably for shots 1 to 17, where the charge size was less than 30 pounds equivalent. No attempt was made to obtain rotation measurements for shots 18 to 25 because of damage to the scribes during previous tests. The scribes were replaced, but failed to operate for shots 26 to 32. These shots varied from 30 to 42.3 pounds equivalent, and it is believed that the blast pressure acted between the torsion springs (Fig. 1) and pushed them outward sufficiently to keep the scribes from functioning.

The impulse imparted to the wheels was calculated from the spring rotation, using both conservation of energy and conservation of momentum. Ignoring gravitational effects in calculating the energy imparted to the system (which represents 1 percent to 3 percent), the energy is given by

$$E = K\,\theta\text{max}\left(\theta\text{p} + \frac{\theta\text{max}}{2}\right) \tag{1}$$

where
- E = energy absorbed into the system (inch-pounds)
- K = spring constant (inch-pounds/radian)
- θmax = maximum spring rotation (radians)
- θp = preload angle to simulate operational roller weight (radians).

24
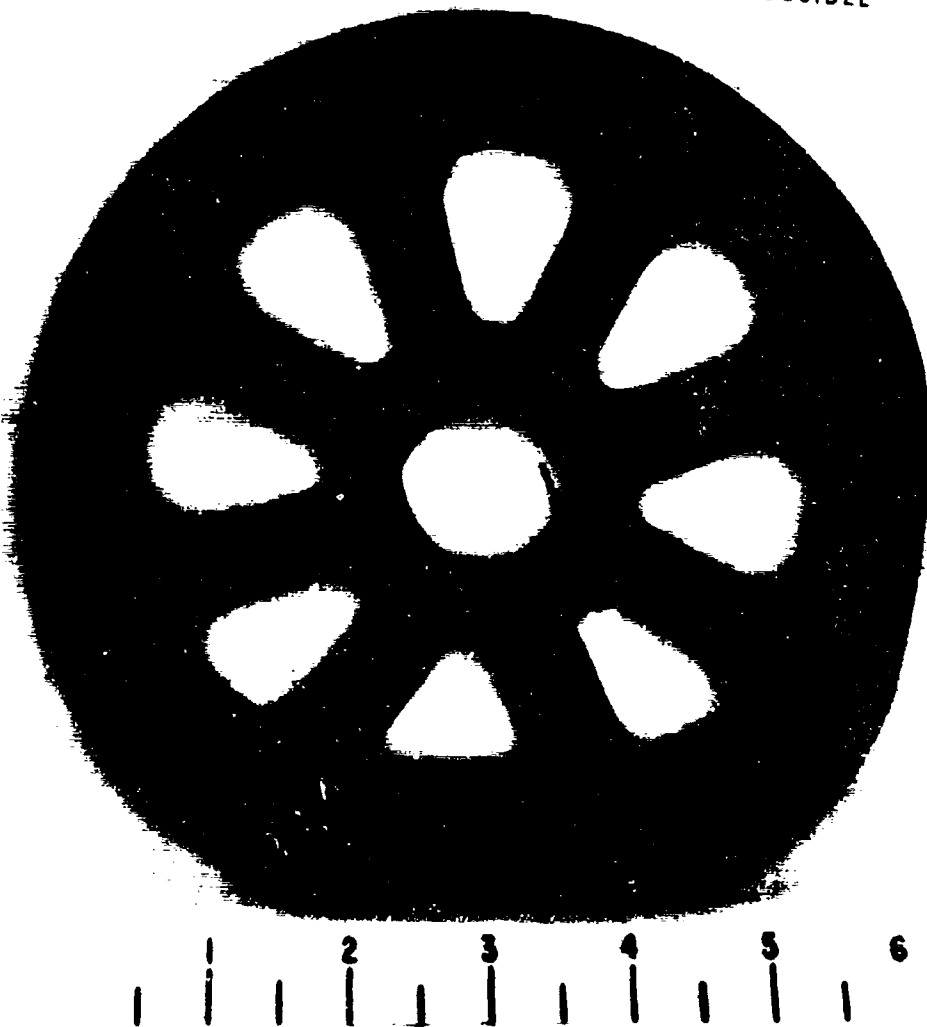
T5564

Fig. 15. 4330 cast wheel showing deformation and rim crack.

T5566

Fig. 16. Crack in rim of cast 4330 wheel.
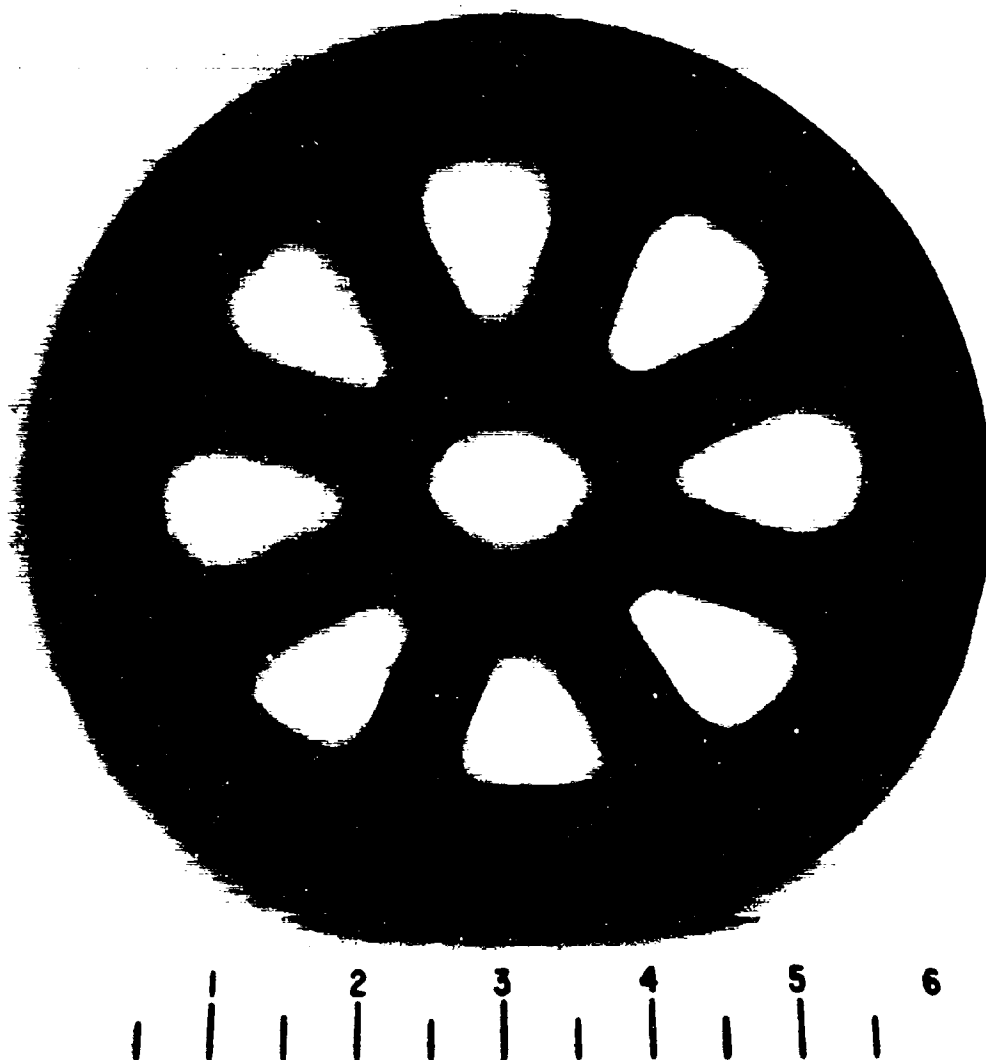
T5565

Fig. 17. General deformation and rim spall of T-1 cast wheel.
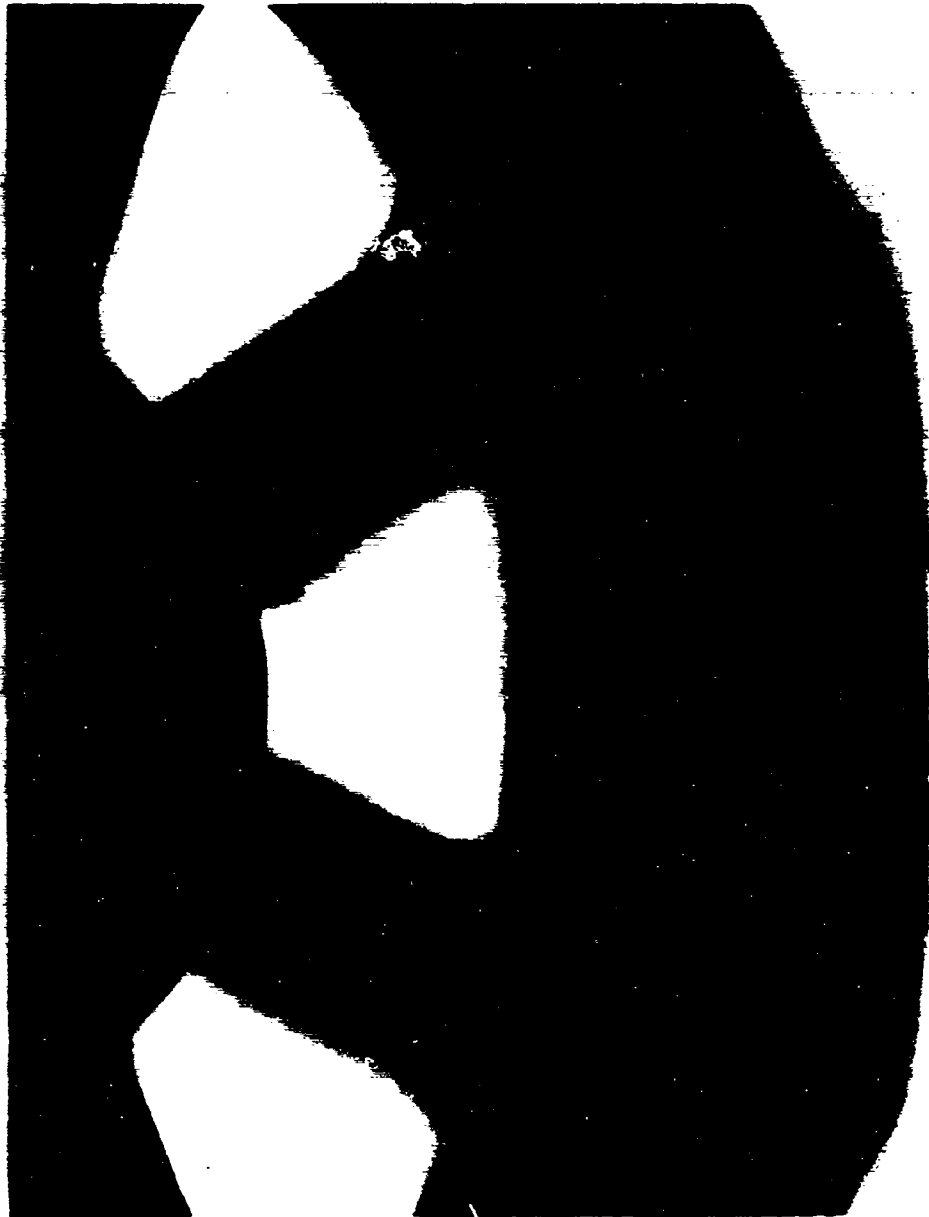
T5567

Fig. 18. Rim spall on T-1 cast wheel.

28
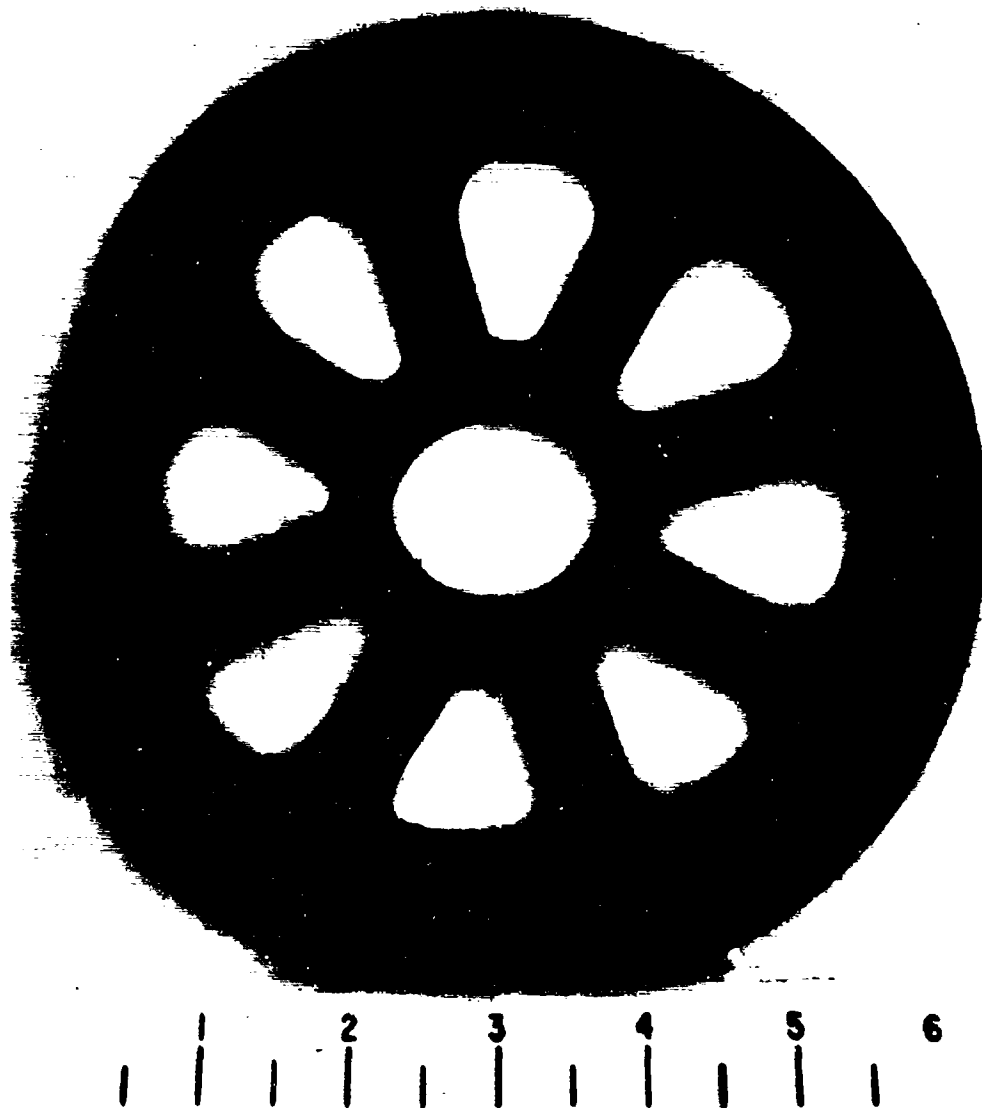
T5568
Fig. 19. General deformation of HY-100 cast wheel.

Conservation of energy and the impulse-momentum relationship yield

$$i = \frac{\sqrt{2KI}}{L}\ \theta max\ \sqrt{1 + \frac{2\theta p}{\theta max}} \tag{2}$$

where   i = impulse (lb-sec)
         I = mass moment of inertia
         L = length of yoke.

The conservation of momentum method also ignores gravitational effects and begins with the basic equation

$$T = I\ddot{\theta} \tag{3}$$

where   T = applied torque
         $\ddot{\theta}$ = angular acceleration.

The equation is solved and boundary conditions of $\theta = 0$ and $\dot{\theta} = \dot{\theta}_{orig}$ at time = 0 are used to evaluate the constants. Rearranging yields the same expression for impulse as given in eq. (2). Complete derivation of these equations is given in Appendix D.

Equations (1) and (2) were used to calculate the energy and impulse imparted to the test system, and these results are presented in Table V. The scaled impulse (impulse divided by the cube root of the charge weight in pounds) and the scaled distance (distance from the charge in feet divided by the cube root of the charge weight in pounds) were calculated, and this scaled-impulse-versus-scaled-distance relationship is shown in Fig. 20.

The majority of tests in Table V are for the three-wheel test configuration. The impulse imparted to the center wheel is estimated by

$$i_c + 2i_c \sin \theta = i_{3\ wheel} \tag{4}$$

where i_c = impulse on center wheel .
         $\tan\theta = 12d/1.75$
         d   = depth to center of charge (feet).

Comparison of values obtained here with shots 14 to 16 indicates that Eq. (4) proportions the impulse appropriately.

30

Table V. Energy and Impulse Imparted to Scale-Model Wheels

Shot Number	Wheel Material and Configuration	Number of Wheels in Test Rig	Equivalent Charge Wt. (lb)	Model Energy (lb-in.)	Prototype Energy (lb-in.)	Model Impulse (lb-sec)	Prototype Impulse (lb-sec)	Scaled Distance (ft/lb$^{1/3}$)	Scaled Distance (lb-sec/lb$^{1/3}$)
2	T-1, flat rim	3	14.7	1790	114,500	23.6	94.4	0.068	38.6
3	T-1, flat rim	3	18.2	3470	222,000	33.0	132.0	0.062	50.2
4	4340, flat rim	3	6.8	1125	72,000	18.8	75.2	0.088	37.7
5	4340, flat rim	3	12.8	2480	158,800	27.8	111.2	0.072	47.5
6	4340, flat rim	3	18.2	2660	170,500	28.8	115.2	0.062	43.8
8	4340, flat rim	3	26.8	9250	592,000	54.8	219.2	0.056	73.3
9	T-1, curved rim	3	18.2	2610	167,000	28.5	114.0	0.062	43.3
10	T-1, curved rim	3	24.3	6110	391,300	43.5	174.0	0.058	60.0
11	4340, curved rim	3	26.8	7250	464,000	47.6	190.4	0.056	63.6
13	4340, curved rim	3	30.0	17,000	1,088,000	72.8	291.2	0.054	93.7
14	4340, flat rim	1	18.2	1140	73,000	14.0	56.0	0.062	21.3
15	4340, flat rim	1	21.8	1550	99,200	16.3	65.2	0.060	23.3
16	4340, flat rim	1	27.4	3280	210,000	23.8	95.2	0.057	32.5

31
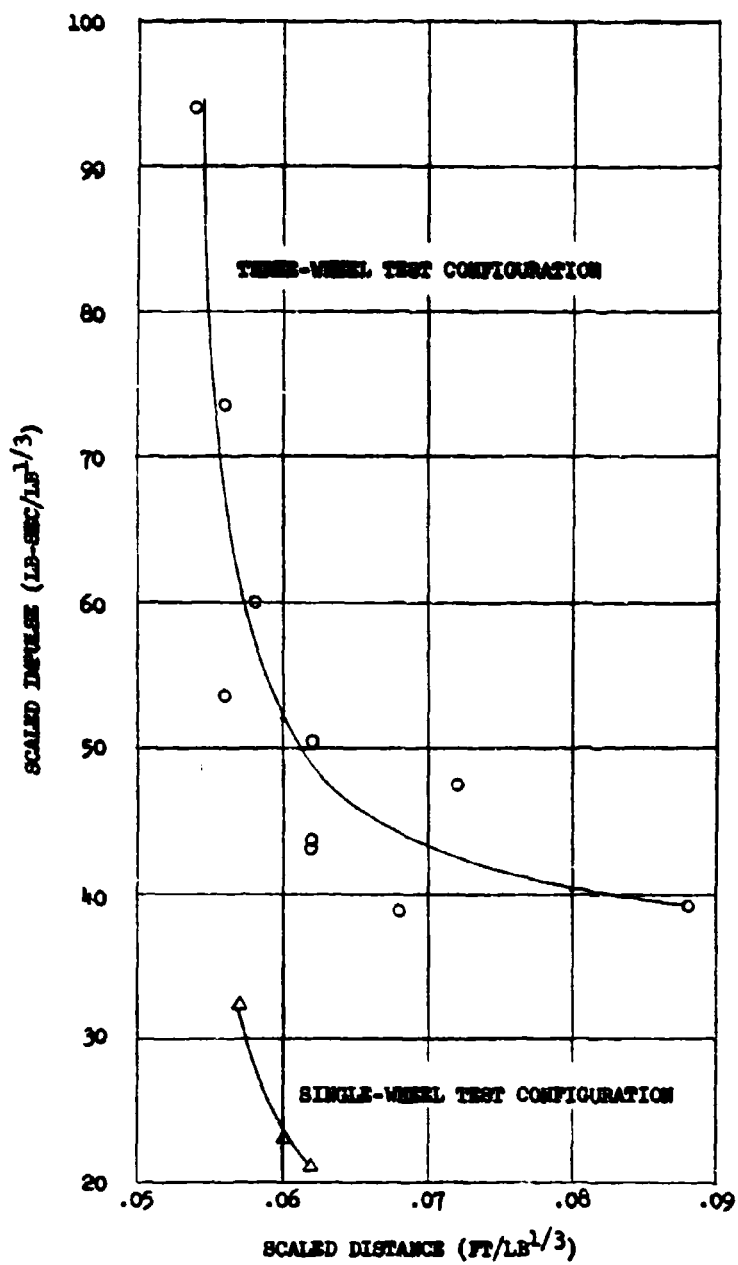
Fig. 20. Scaled impulse versus scaled distance for test charges.

32

Westine[2] has developed a method of calculating the impulse imparted to a target from a land mine detonation given by

$$I = iA \theta \qquad (5)$$

where
I = total impulse
i = specific impulse
A = projected area = 2rh = 7 in.[2] for the test wheels
θ = shape factor, which is a function of target shape and standoff conditions.

Westine's paper determines this shape factor for the various configurations tested under this program. These shape factors, together with the impulse imparted to the center wheel, as calculated by eq. (4), are used to calculate the specific impulse generated by the detonations. This impulse is transformed to scaled specific impulse by dividing by the cube root of the charge weight and is presented in Table VI. These values are compared to previous data[3], as extrapolated for surface-emplaced charges, in Fig. 21. These previous data are for TNT charges and have been adjusted for C-4 explosive. Data generated under this project are seen to fall within the limits of the previous data.

Table VI. Scaled Specific Impulse

Shot Number	Impulse on 1 Wheel (lb-sec)	θ	Specific Impulse (psi-sec)	$\frac{i}{w^{1/3}} \left(\frac{psi\text{-}sec}{Lb^{1/3}} \right)$
2	12.1	4.30	0.402	656
3	16.1	4.00	0.575	875
4	10.7	5.45	0.281	594
5	14.6	4.55	0.457	782
6	14.1	4.00	0.504	766
8	24.2	3.25	1.063	1420
9	13.9	4.00	0.496	755
10	20.1	3.40	0.845	1165
11	21.4	3.25	0.942	1260
13	31.7	3.10	1.460	1880
14	13.7	4.00	0.489	744
15	15.9	3.60	0.631	900
16	23.9	3.40	1.005	1370

[2]Peter S. Westine, "The Impulse Imparted to Targets by the Detonation of Land Mines," (paper to be presented at the AOA Countermine Symposium, 24-25 March 1971).

[3]W. D. Kennedy, "Explosions and Explosives in Air," in *Effects of Impact and Explosions*, Volume I, Summary Technical Report, NDRC, Washington, 1946.
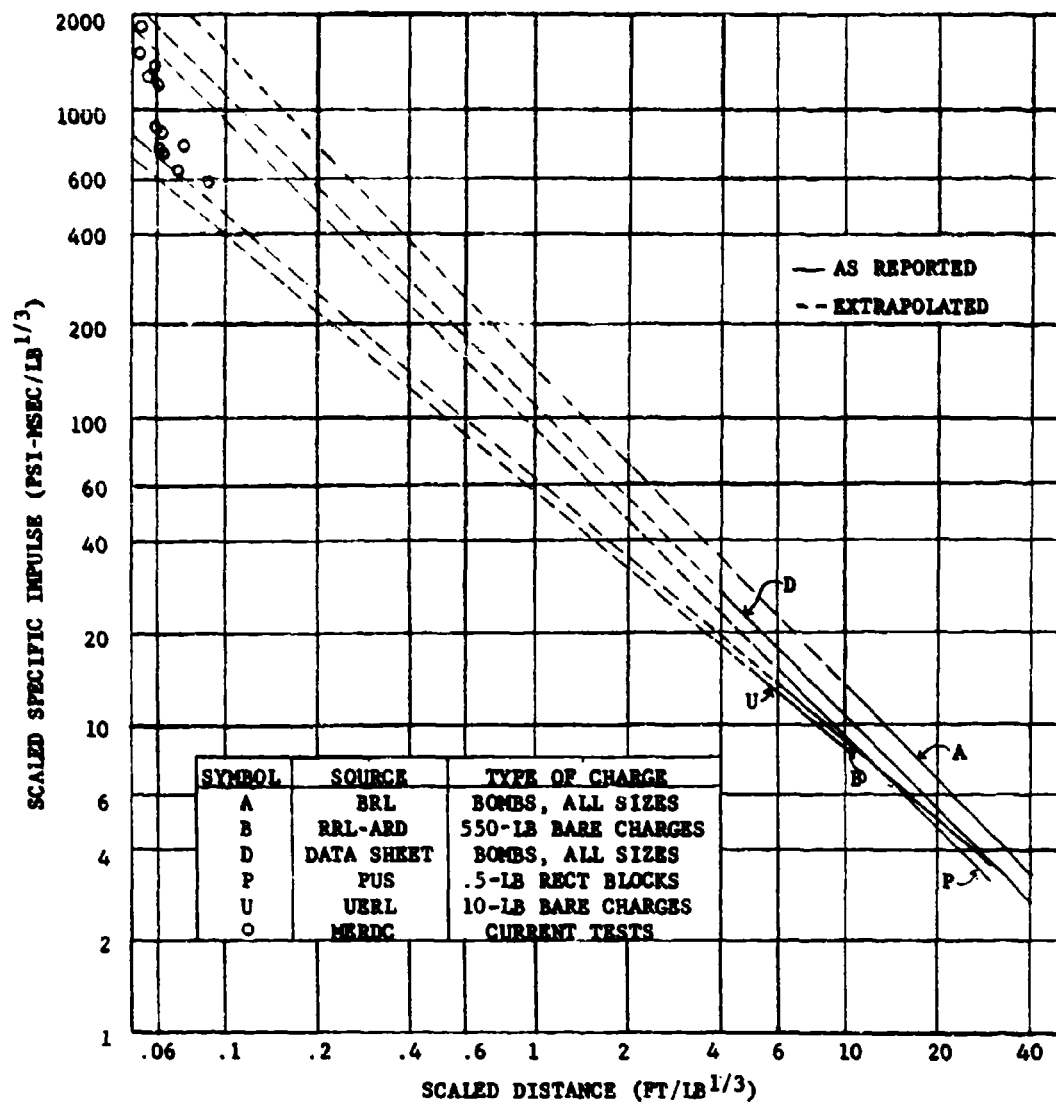
Fig. 21. Scaled specific impulse versus scaled distance from various sources.

10. Cratering Effects. The radii of the craters resulting from 18 of the test shots were measured and are presented in Table VII, along with two scaling factors ($\frac{R}{d}$ and $\frac{W^{1/3}}{d}$, where d = burial depth and R = crater radius). Westine[4] suggests an approximate method of evaluating and predicting explosive cratering effects, and the current data are compared to previous tests[4,5] in Fig. 22. The current tests and those in Ref. 5 were conducted in a clayey, sandy soil, and those in Ref. 4 in a desert alluvium.

Table VII. Cratering Effects

Shot Number	Crater Radius (in.)	$\frac{R}{d}$	$\frac{W^{1/3}}{d}$ $\left(\frac{lb^{1/3}}{ft}\right)$
1	4.5	9.0	11.75
5	16.0	32.0	14.05
6	15.0	30.0	15.80
7	13.0	26.0	16.80
8	14.0	28.0	17.90
11	14.5	29.0	17.90
12	15.5	31.0	18.70
13	18.5	37.0	18.70
14	15.5	31.0	15.80
15	16.0	32.0	16.80
16	15.5	31.0	17.60
18	17.0	34.0	17.30
19	17.5	35.0	18.00
20	17.0	34.0	18.70
21	18.5	37.0	18.70
22	18.0	36.0	18.70
27	17.5	35.0	19.60
28	17.5	35.0	20.40

11. Effects of Rim Curvature. Rounding the rim on the machined wheels, as in Fig. 8, increased the blast resistance of these wheels by an average of 30 percent. The T-1 flat-rimmed wheels withstood the equivalent of 14.7 pounds of explosive without cracking, but cracked under 18.2 pounds equivalent. The T-1 curved-rim wheel

[4]Peter S. Westine, "Explosive Cratering," Journal of Terramechanics, 7, No. 2, pp. 9-19. Pergamon, London.

[5]USAMERDC, "Preliminary Experiments for Crater Modeling in Controlled Soil Media," Technical Report 1862, Fort Belvoir, Virginia, June 1966.

Fig. 22. Scaled crater radius versus charge size and burial depth.

36

withstood the 18.2 pounds equivalent, but cracked under the attack of an equivalent of 24.3 pounds of explosive. The increase in blast resistance is measured by dividing 18.2 by 14.7, yielding an increase factor of 1.24.

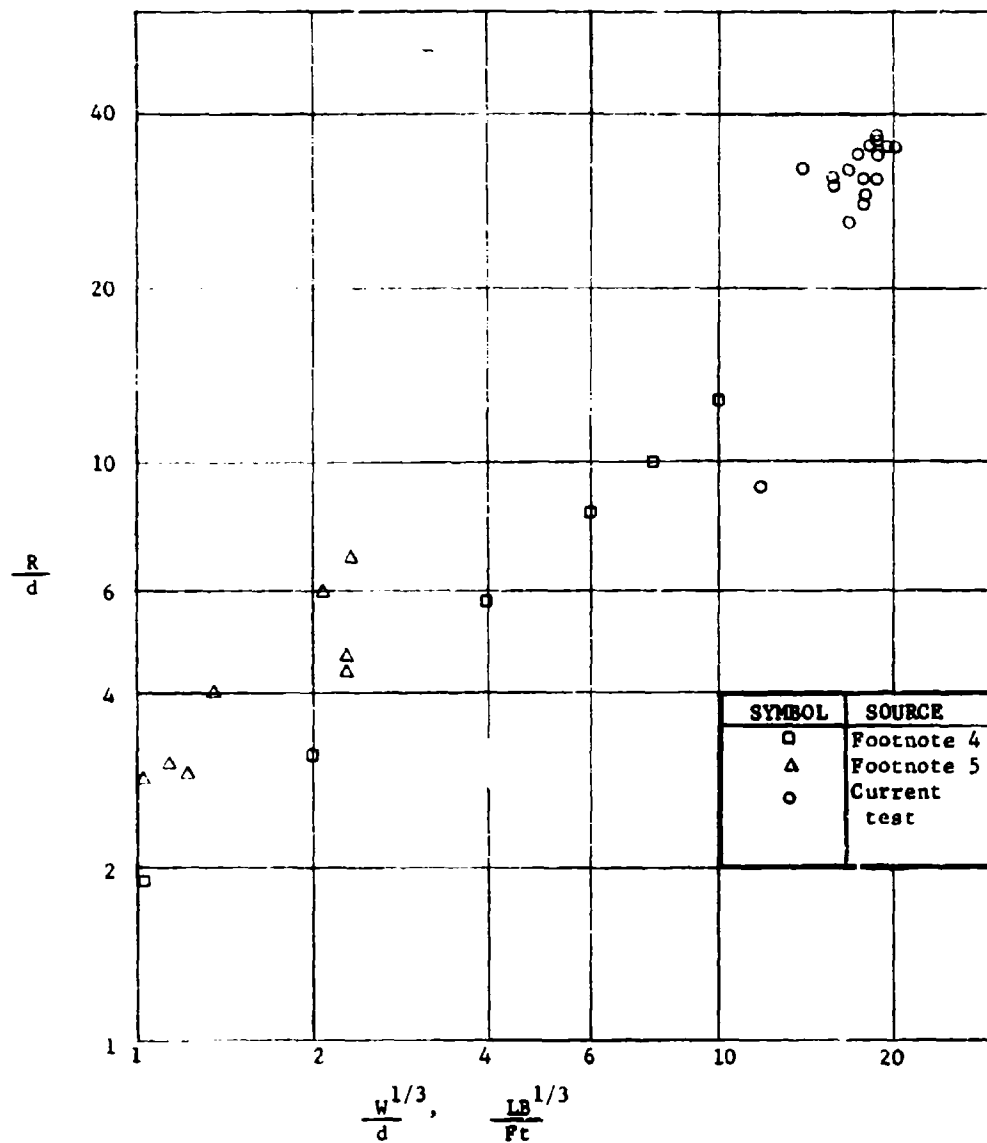The flat-rimmed 4340 wheels withstood the effects of 21.8 prototype pounds of explosive without cracking, but cracked under the equivalent of 26.8 pounds of explosive. The 4340 curved-rim wheel withstood 26.8 pounds equivalent, but cracked under the second shot, equivalent to 30 pounds. The increase factor for these wheels is 1.37 (30 divided by 21.8).

The cast wheels were rounded more than the machined ones and resulted in a 1-percent increase in blast resistance over the machined wheels. Both the T-1 and HY-10C wheels withstood blasts of 35 pounds, but cracked or suffered excessive deformation under the equivalent of 39.5 pounds of explosives. The 4330 wheel withstood two blasts equivalent to 30 pounds and cracked slightly under a third 30-pound prototype charge. It is felt that this wheel would have also withstood a prototype 35-pound shot. These tests yield an increase factor of $\frac{35}{30} = 1.17$.

In all of the above cases, plastic deformation of the rim decreased as the wheels became more rounded. Rim widening of the flat-rimmed wheels was excessive even at low charge weights. The cast wheels suffered little widening at higher charge levels. This plastic deformation is critical because of the necessity of designing yokes and other components to accept a maximum-width wheel. Diameter changes produced in the wheels by the blasts were similar in proportion to the rim widening.

12. **Effects of Material Selection.** The higher carbon content of 4340 over T-1 would indicate higher strength levels for the former. 4340's higher nickel content would also suggest higher ductility and fracture toughness. Table II verifies the differences in yield and tensile strengths, but indicates that the elongation of the 4340 is considerably below that of the T-1. This 4340 elongation would suggest premature brittle fracture, but this was not observed. The 4340 steel gave the wheels a 48-percent blast resistance increase (21.8 pounds versus 14.7 pounds, and 26.8 pounds versus 18.2 pounds for the flat and curved rims, respectively) over the T-1 machined steel.

The nonlaminar structure of cast steel would suggest that cast wheels are preferable to the machined product. Both the cast T-1 and HY-100 wheels failed at 39.5 pounds of explosive equivalent, the T-1 by cracking (Figs. 17 and 18), and the HY-100 by excessive deformation (Fig. 19). These wheels withstood blasts of 35 pounds equivalent, and thus represent a blast resistance increase of 92 percent (35 pounds prototype versus 18.2 pounds, or $\frac{35}{18.2} = 1.92$) over the T-1 machined wheel (curved rim) and an increase of 138 percent (35 pounds prototype versus 14.7 pounds, or $\frac{35}{14.7} = 2.38$) over

37

the flat-rimmed T-1 wheel. The 4330 cast wheel would have withstood an equivalent 35-pound charge, for an increase of 138 percent over the T-1 flat-rimmed wheel, but its more desirable chemical composition and its ease of procurement make it more desirable than either T-1 or HY-100.

IV. CONCLUSIONS

13. Conclusions. Within the limits of this program, it is concluded that:

    a.   The blast resistance of machined, curved-rim wheels (radius of rim curvature equals one-fourth of the wheel width) is approximately 25 percent better than that of flat-rimmed wheels of the same material (T-1 and 4340 steels).

    b.   Cast 4330, HY-100, and T-1 curved-rim wheels (radius of rim curvature equals two-fifths of the wheel width) provide a 138-percent blast resistance increase over the machined T-1 flat-rimmed wheels; the 4330 is desirable because of its better chemical and mechanical properties and its lower production cost.

    c.   Cast steel appears to be a better candidate material than machined steel because of the former's nonlaminar internal structure and its relative ease and low cost of quantity production.

    d.   Qualitative data generated by these tests indicate that the full-scale design may be practical and will satisfy the blast-resistance requirements.

    e.   Data generated on scaled specific impulse for scaled distances of 0.05 to 0.09 ft/lb$^{1/3}$ are seen to agree with extrapolated data obtained in the 4 to 50 scaled distance range.

APPENDIX A

PRELIMINARY REPORT ON OPTIMUM WHEEL CONFIGURATION TESTING FOR MINE CLEARING ROLLERS, 10 MARCH TO 9 JUNE 1970

SUMMARY:

The draft proposed QMR for a Vehicle-mounting, Nonexpendable Mine Clearing System specifies that mine clearing efficiency is to be based upon the M-15 mine buried such that the pressure plate is 6 inches below the soil surface. This limited project was conducted to experimentally determine the optimum wheel width, diameter, and spacing to clear these mines. This optimum configuration will, in turn, be dependent on the load transfer efficiency, defined as the load on a buried simulated M-15 pressure plate divided by the wheel load at ground level and on the rolling resistance of the wheels.

The report concludes that:

1. For clearing speeds of 5-mph, 22-inch-diameter, 3-inch-width wheels spaced at 6-inch centers produced the highest load transfer efficiency in the sand and clay tested, but the same wheels spaced at 8-inch centers required the lowest operational roller load due to the fewer wheels required.

2. For a given wheel load, the rolling resistance appeared to be dependent primarily on the wheel width and on the number of wheels required for an operational roller. The experimentally determined wheel sinkages were practically independent of the wheel width and diameter.

BACKGROUND:

A computer study based on applications of the Boussinesq equation for vertical stresses in soils was conducted to determine the pressure bulb created under each of the 20 combinations of wheel diameter and width. Using these data, the pressure isobars under a single wheel and under a pair of wheels were constructed and are shown in Fig. 23. Narrower, smaller diameter wheels produce higher pressures but have higher rolling resistances than wider, larger diameter wheels. As seen in Fig. 23b, the lowest pressure is between the two wheels, and the intensity of this pressure is dependent on the wheel spacing. Closer spaced wheels yield higher pressure for a given wheel load, but this advantage is offset by the increased number of wheels required. Based on these data, wheels of 22- and 30-inch diameters with 3- and 4-inch widths each, spaced at 6- and 8- or 8- and 10-inch centers for the 3- and 4-inch widths, respectively, were selected for testing

a. Single Wheel   b. Pair of Wheels
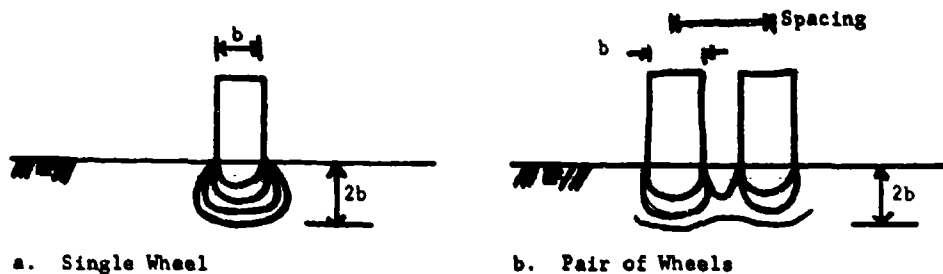
Fig. 23. Theoretical pressure distributions.

TEST PROCEDURE

The M113 Armored Personnel Carrier and the APC mounted roller were used as the
basic items of test hardware. The original ten aluminum wheel arm assemblies were
removed from the roller, and two steel arms and wheels were placed on each bank as
shown in Fig. 24. The wheel articulation bellows were inflated to 180 psig to provide
wheel articulation and the weight transfer bellows were not inflated as this combina-
tion produced an average wheel load of 1750 pounds. Additional pressure in the
weight transfer bellows would overload the test arms.
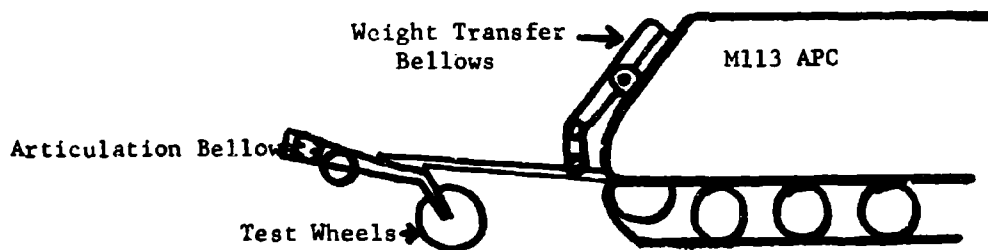
Fig. 24. M113 APC Roller as test hardware.

Baldwin-Lima-Hamilton load cells (type U-1, 5000-pound capacity) were used to mea-
sure the load under the soil. The cells were fitted with base plates for stability and with
7-inch-diameter pressure plates to simulate the M-15 pressure plate. The cells were
buried as shown in Fig. 25. The roller was driven across the load cells so that the two
experimental wheels on a bank were equidistant from the center of the cell, per Fig. 23b.
The loads on the cells were recorded on a Honeywell Visicorder (two-channel), and the

40
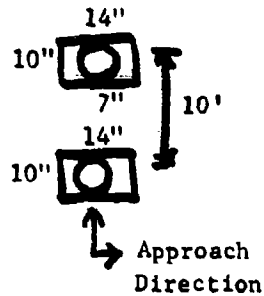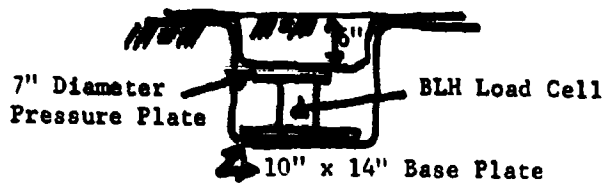
Fig. 25. Cell burial.

time between impulses for the first and second cells was used to determine vehicle speed. The soil above the cells was reworked after each run to provide uniform initial conditions.

The load on the wheel at ground level was measured by driving one experimental wheel onto a hydraulic load cell positioned on a support plate so that the top of the cell was at ground level. The wheel was stopped on the center of the cell, and the load was recorded in this position.

RESULTS AND DISCUSSION

All tests were run at an aveage speed of 5 mph in dry construction sand in the covered test lane at Range 5 and in moist rocky clay on Range 1, EPG. The experimentally determined load transfer efficiencies for these conditions are presented in Table VIII. Calculations based on the pressure isobars of Fig. 23b suggest a maximum load transfer efficiency of .65 at 6-inch burial depth for the stationary condition. Allowing a 70-percent impact factor for the wheels dropping into the looser soil above the cell, a maximum transfer efficiency of 1.1 is theoretically possible. Thus, some of the experimental data conflicts with theory with respect to data magnitude and further testing must be performed to confirm these data.

A total width of 160 inches is assumed for an operational roller. The total roller assembly ground load for such a roller is, therefore, a function of the load on the target required to actuate it, the transfer efficiency of the wheel configuration, and the number of wheels required. Thus,

$$\text{Total Load} = (\text{Load to actuate}) \times \left(\frac{1}{\text{Trans. eff.}}\right) \times (\text{No. of wheels})$$

or

41

Total Load = (Load to actuate) x (Load trans. factor)

These transfer factors are presented in Table IX.

Theory of Land Locomotion by Bekker gives the sinkage and rolling resistance of a wheel in soil as

$$z_o = \left(\frac{3W}{Kb\sqrt{D} \ (3-m)} \right)^{\frac{2}{2m+1}} \quad \text{and} \quad RR = Kb \frac{z_o^{m+1}}{m+1}$$

where

z_o = wheel sinkage, inches RR = rolling resistance

W = wheel load, pounds K, m = soil properties

b, D = wheel width, diameter

In conflict with theory, the experimental wheel sinkages were found to be practically independent of wheel dimensions for a given load. With this constant sinkage and a given soil, the total rolling resistance for an operational roller appears to be dependent on the wheel width and number of wheels. This rolling resistance is given by

$$\text{Total rolling resistance} = (\text{Wheel width}) \times (\text{No. of wheels}) \times \left(K \frac{z_o^{m+1}}{m+1} \right)$$

or

$$\text{Total rolling resistance} = (\text{Rolling resistance factor}) \times \left(K \frac{z_o^{m+1}}{m+1} \right)$$

These rolling resistance factors are given in Table X.

CONCLUSIONS

The 22-3-8 wheel configuration requires the lowest total roller assembly ground load and appears to produce the least total rolling resistance. These data are based on a limited number of tests and conditions and conflicts with theoretical work in several areas. Further testing to verify these data and to extend it to other soils must be done before the determination of the optimum mine clearing roller wheel configuration can be made from these data alone.

42

Table VIII. Transfer Efficiencies

Wheel Diameter (In.)	Wheel Width (In.)	Wheel Spacing (In.)	Transfer Efficiency (Sand)	Transfer Efficiency (Clay)
22	3	6	1.17	1.27
22	3	8	0.97	1.02
22	4	8	0.79	1.16
22	4	10	0.52	*
30	3	6	0.92	1.07
30	3	8	0.88	0.75
30	4	8	0.72	0.77
30	4	10	0.58	*

*Not tested because of poor showing in initial testing.

Table IX. Load Transfer Factors

$$\text{Load transfer factor} = \frac{1}{\text{Trans. Eff.}} \times (\text{No. of wheels})$$

Wheel Configuration	No. of Wheels Required	Transfer Factor (Sand)	Transfer Factor (Clay)	Transfer Factor (Avg.)
22-3-6*	27	23.1	21.2	22.15
22-3-8	21	21.6	20.6	21.1
22-4-8	21	26.6	18.1	22.35
22-4-10	17	32.7	**	32.7
30-3-6	27	29.4	25.2	27.3
30-3-8	21	23.8	28.0	25.9
30-4-8	21	29.2	27.3	28.25
30-4-10	17	29.4	**	29.4

*Diameter-Width-Spacing.

**Not Tested.

Total roller assembly ground load = (Load to actuate) x (Load transfer factor)

Table X. Rolling Resistance Factors

Rolling resistance factor = (Wheel width) x (No. of wheels)

Wheel Configuration	Rolling Resistance Factor
22-3-6*	81
22-3-8	63
22-4-8	84
22-4-10	68
30-3-6	81
30-3-8	63
30-4-8	84
30-4-10	68

*Diameter-Width-Spacing

APPENDIX B

DERIVATION OF SCALING LAWS GOVERNING BLAST PHENOMENA*

Physical Parameters

Symbol	Description	Units
P	Blast pressure	FL^{-2}
t	Time	T
ρ	Mass density of soil	$FL^{-4}T^2$
c	Seismic velocity of soil	LT^{-1}
L	Characteristic length	L
r_i	Shape of system	————
M	Mass of wheel	$FL^{-1}T^2$
g	Acceleration of gravity	LT^{-2}
f	Total load on wheel	F
E	Energy absorbed in wheel system	FL
a	Acceleration of wheel under blast	LT^{-2}
I	Impulse applied to wheel	$FL^{-2}T$
σ	Stress in wheel	FL^{-2}

---

*Method after "A Seminar on Modeling Weapon Effects," W. E. Baker et al, Southwest Research Institute.

Derivation of Pi Terms

The above parameters are arranged in matrix form with M, L, and P as the dimensionally independent variables.

	P	L	M	t	ρ	c	r_i	g	f	E	a	l	σ
F	1	0	1	0	1	0	0	0	1	1	0	1	1
L	-2	1	2	0	-4	1	0	1	0	1	1	-2	-2
T	0	0	-1	1	2	-1	0	-2	0	0	-2	-1	0

An identity submatrix of the independent parameters is first developed by applying appriate matrix operations. Such a submatrix is shown below:

	PL^2	L	$\left(\dfrac{M}{LP}\right)^{1/2}$	t	ρ	c	r_i	g	f	E	a	l	σ
F	1	0	0	0	1	0	0	0	1	1	0	1	1
L	0	1	0	0	-4	1	0	1	0	1	1	-2	-2
T	0	0	1	1	2	-1	0	-2	0	0	-2	1	0

This matrix indicates that if ρ is divided by PL^2, the resulting expression $\dfrac{\rho}{PL^2}$ will not contain the force dimension. If this expression is then multiplied by L^4, the resulting expression contains neither force or length dimensions. If this expression is divided by $\dfrac{M}{LP}$, the resulting expression $\dfrac{PL^3}{MP}$ will be dimensionless. This procedure can be followed to produce a matrix of dimensionless products, as shown below:

	PL^2	L	$\left(\dfrac{M}{LP}\right)^{1/2}$	$\left(\dfrac{t}{\frac{M}{LP}}\right)^{1/2}$	$\dfrac{PL^2}{MP}$	$\dfrac{cM^{1/2}}{L^{3/2}P^{1/2}}$	r_i	$\dfrac{gM}{L^2P}$	$\dfrac{f}{PL^2}$	$\dfrac{E}{PL^3}$	$\dfrac{aM}{L^2P}$	$\dfrac{lL^{1/2}}{P^{1/2}M^{1/2}}$	$\dfrac{\sigma}{P}$
F	1	0	0	0	0	0	0	0	0	0	0	0	0
L	0	1	0	0	0	0	0	0	0	0	0	0	0
T	0	0	1	0	0	0	0	0	0	0	0	0	0

APPENDIX C

METALLURGICAL ANALYSIS OF WHEEL AND YOKE STEEL CASTINGS

Prepared by Howard E. Horner, Materials Research Support Division, USAMERDC

1.   The purpose of this work was to conduct metallurgical analysis on steel castings made in the foundry at the Naval Research Laboratories. These castings were reduced-size wheels and yokes to be subjected to explosive testing in a scaled-down material test program for nonexpendable mine clearing roller components. Chemical analysis, mechanical tests and radiographic examination were performed on the castings made from three recommended nickel steel alloys: 4330, T-1, and HY-100. Three wheels and three yokes were to be made from each alloy, a total of 18 castings.

2.   The samples for chemical analysis of each steel alloy were obtained from rectangular test coupons which were cast with the yokes. These coupons were not heat treated. The chemical analysis was conducted in accordance with Federal Test Method Standard No. 151b:

    Test Method 111.2 "Chemical Analysis" using the combustion method for determination of carbon and sulfur contents.

    Test Method 112.2 "Spectrochemical Analysis" using A.C. Arc emission spectrographic method for determination of boron content and x-ray fluorescence spectrometric method for determination of other element contents.

    The mechanical properties of the steel castings were determined from tensile, impact, and hardness tests performed on the test coupons. These tests were conducted in accordance with American Society for Testing and Materials Specification ASTM A370 "Standard Methods and Definitions for Mechanical Testing of Steel Products."

    The tensile specimens were obtained from double keelblock coupons cast separately. These coupons were heat treated before being machined into standard 1/2-inch round tensile test specimens with 2-inch gage length and threaded ends. The tensile tests were carried out on a 300,000-pound rated-load-capacity Baldwin Universal Testing Machine. A 2-inch gage length extensometer was tested to automatically record the load-strain curve of each tensile specimen.

47

The Charpy V-notch impact specimens were machined from heat-treated test coupons which were cast with the yokes. The impact tests were performed at room temperature on a Sonntag universal impact machine using a 120-ft/lb range.

The hardness measurements were made on heat-treated tensile and impact specimens after they were tested.

Radiographic examination of the steel castings was conducted in accordance with ASTM E-94, "Recommended Practice for Radiographic Testing," and ASTM E-142, "Controlling Quality of Radiographic Testing." The radiographs of the castings were obtained using the General Electric OX-250 industrial radiographic unit and type AA industrial x-ray films with and without lead screens.

3.   The composition and mechanical properties of the steel castings analyzed are presented in Table XI. Two heats of 4330 steel alloy were made when one of three wheels cast from the first heat was defective because of excessive trapped slag on the surface of the wheel. Therefore, four wheels were made from 4330 steel alloy, two wheels per heat. All the heats except T-1 steel alloy were within the specified chemical composition. The boron content in the T-1 heat was above the maximum specified content.

The castings and test coupons were heat treated in accordance with the recommended heat treatment given in Table XII for each steel alloy. A minimum yield strength of 100,000 psi was obtained for heat-treated 4330 and HY-100 steel castings. However, the tensile properties of heat-treated T-1 castings were much higher than desired. The cause for higher tensile properties in T-1 castings may be due to high boron content. Boron is a powerful hardening alloying element in steel. The tensile properties can be lowered to the desired level by retempering the T-1 castings to 1250° F for one hour. Nevertheless, the T-1 castings will be tested in the material test program with their high tensile properties.

The radiographs indicated that most castings did not meet the requirements of class 2 castings of ASTM E-71, "Reference Radiographs for Steel Castings up to 2 Inches in Thickness," because of excessive internal shrinkage and some large gas holes. These castings, however, were accepted for use in the material test program because of the amount of time involved in making more castings to meet class 2 radiographic rating.

4.   It is concluded that:

a.   The chemical composition of tne castings were in accordance with the requirements as specified, except for the T-1 steel which had a higher boron content than required.

48

Table XI. Composition and Mechanical Properties of Steel Castings

Steel Castings	ASTM A487 Heat 1	Class 10Q (4330) Heat 1A	MIL-S-23008 (HY-100) Heat 2	ASTM A487 Class 7Q (T-1) Heat 3
A. Composition				
Carbon	0.27%	0.27%	0.21%	0.17%
Manganese	0.71	0.94	0.68	0.81
Nickel	1.75	1.80	3.15	0.83
Chromium	0.63	0.78	1.49	0.55
Molybdenum	0.30	0.35	0.49	0.58
Vanadium	—	—	—	0.07
Copper	0.03	0.04	0.02	0.33
Sulfur	0.02	0.02	0.02	0.03
Boron	—	—	—	<0.009
B. Properties				
Tensile strength, psi	128,094	129,797	121,520	151,928
Yield strength, psi	113,285	110,833	102,640	139,699
Elongation, %	18.2	18.0	16.2	10.9
Reduction of area, %	46.1	45.0	44.5	41.3
Hardness, Rc	27.5	29.5	26.5	35.5
Charpy impact (V-notch), ft/lb	26.5	42.0	23.5	14.0

NOTE: A. The yield strength was determined at 0.2% offset of load-strain curve.

B. Elongation was determined in 2 inches of gage length. The elongations were somewhat approximations because many tensile specimens failed near or at the gage length marks.

C. Charpy impact tests were conducted at room temperature of 72° F.

D. The steel castings were heat treated in accordance with heat treatment recommendations listed in Table XII.

E. Mechanical properties were the averaged results of three determinations for the mechanical tests.

F. The dimension to bottom of notch of the impact specimens varied considerably with each heat, thus making evaluation of the impact tests difficult to interpret. The specified dimension to bottom of notch for Charpy V-notch impact test specimen is 0.315 ±0.001 inch. The dimension of the specimens used in the impact tests were as follows:

Heat 1	—	0.3115 inch
Heat 1A	—	0.3140 inch
Heat 2	—	0.3095 inch
Heat 3	—	0.2850 inch

49

Table XII. Recommended Heat Treatments for Steel Castings

ASTM A487, Class 10Q (4330)	— A.	Normalize at 1650° F for 1 hour and then cool in air
	B.	Austenitize at 1550° F for 1 hour and then quench in water.
	C.	Temper at 1150° F for 2 hours.
MIL-S-23008 (HY-100)	— A.	Normalize at 1800° F for 1 hour and then cool in air.
	B.	Austenitize at 1550° F for 1 hour and then quench in water.
	C.	Temper at 1150° F for 2 hours and then quench from tempering temperature.
ASTM A487, Class 7Q (T-1)	— A.	Normalize at 1750° F for 1 hour and then cool in air.
	B.	Austenitize at 1550° F for 1 hour and then quench in cold water.
	C.	Temper at 1150° F for 2 hours.

b. The mechanical properties of the heat-treated 4330 and HY-100 steel castings were satisfactory. The tensile properties of the heat-treated T-1 castings were much higher than desired which may be due to high boron content.

c. Most castings did not meet the radiographic requirements of class 2 of ASTM E-71 because of excessive internal shrinkage and some large gas holes. These castings, however, were accepted for use in the material test program in order to obtain necessary data as soon as possible from the explosive tests.

5. It is recommended that:

a. The soundness of the steel castings be improved by using better gating and riser system in the sand molds in order to minimize internal shrinkage. Defects in the castings can act as notches, setting up high stress concentrations which could cause early failure of the wheel and yoke castings when they are subjected to high loading type of service.

b. The tensile properties of T-1 castings should be lowered by retempering in order to obtain valid comparison at the same tensile level with 4330 and HY-100 steel castings.

50

DERIVATION OF IMPULSE EQUATION

Conservation of Energy Method
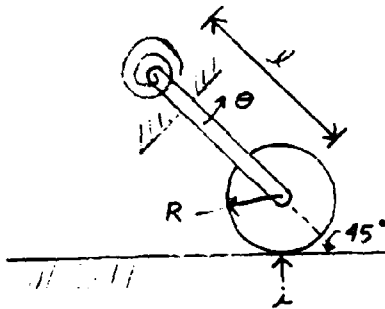
Symbol	Description
θp	preload angle
θmax	maximum rotation
K	spring constant
Wy	weight of yokes
Ww	weight of wheels
i	total impulse
E	total energy

This derivation ignores gravitational effects.

$$E = \text{Force x Distance} = \left[\frac{K}{\ell}\left(\theta p + \frac{\theta max}{2}\right) \right] \times \{\theta max \; \ell\}$$

$$E = K\,\theta max \left(\theta p + \frac{\theta max}{2}\right) \tag{1}$$

From conservation of energy, K.E. = P.E.

$$1/2\, mv^2 = E$$

$$v = \sqrt{2E/m} \tag{2}$$

From the impulse-momentum relationship,

$$\frac{i}{\sqrt{2}} = mv = \sqrt{2Em} \tag{3}$$

Substitution eq. (1) into eq. (3)

51

$$i = \sqrt{4\,m\,K\,\theta_{max}\left(\theta_p + \frac{\theta_{max}}{2}\right)}$$

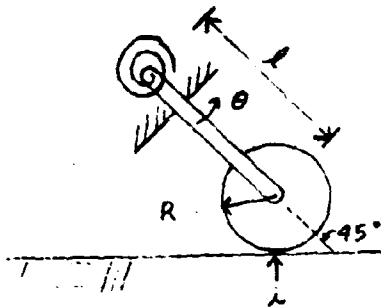$$i = \sqrt{4\,m\,K\,\frac{\theta_{max}^2}{2}\left(\frac{2\theta_p}{\theta_{max}} + 1\right)}$$

$$i = \sqrt{2\,m\,K}\;\;\theta_{max}\;\sqrt{1 + \frac{2\theta_p}{\theta_{max}}}$$

But $l = m\ell^2$ so $m = \dfrac{l}{\ell^2}$.

Thus

$$i = \frac{\sqrt{2\,K\,l}}{\ell}\;\;\theta_{max}\;\sqrt{1 + \frac{2\theta_p}{\theta_{max}}}$$

Conservation of Momentum Method

Symbol	Description
Mo	initial spring moment
K	spring constant
θ	rotation
ℓ	length of yoke
I	mass moment of inertia
i	total impulse
T	torque

This derivation ignores gravitational effects.

$$T = I \ddot{\theta}$$

$$-(Mo + K\theta) = I \ddot{\theta}$$

$$\ddot{\theta} + \left(\frac{K}{I}\right)\theta = - \left(\frac{Mo}{I}\right) \qquad (1)$$

Boundary conditions at t=0 are θ=0 and $\dot{\theta} = \dot{\theta}_{orig}$

$$I \dot{\theta}_{orig} = \frac{\ell}{\sqrt{2}} \; i$$

$$\dot{\theta}_{orig} = \frac{\ell \; i}{\sqrt{2} \; I}$$

For small angles ($\sin \theta = \theta$), the solution of eq. (1) is

$$\theta = A \cos \sqrt{\frac{K}{I}} \; t + B \sin \sqrt{\frac{K}{I}} \; t - \frac{Mo}{K} \qquad (2)$$

$$\dot{\theta} = - A \sqrt{\frac{K}{I}} \; \sin \sqrt{\frac{K}{I}} \; t + B \sqrt{\frac{K}{I}} \; \cos \sqrt{\frac{K}{I}} \; t \qquad (3)$$

Substituting the boundary conditions into eqs. (2) and (3) yields

$$A = \frac{Mo}{K} \qquad \text{and} \qquad B = \frac{\ell \; i}{\sqrt{2KI}}$$

53

θmax occurs at time, t_{max}, when $\dot{\theta} = 0$, or when

$$\tan \sqrt{\frac{K}{I}} \; t_{max} = B/A$$

Calculating sin and cos from tan yields

$$\cos \sqrt{\frac{K}{I}} \; t_{max} = \sqrt{\frac{1}{1 + (B/A)^2}} \quad , \quad \sin \sqrt{\frac{K}{I}} \; t_{max} = \sqrt{\frac{(B/A)^2}{1 + (B/A)^2}}$$

Substituting into eq. (2) to determine θmax,

$$\theta max = A \sqrt{\frac{1}{1 + (B/A)^2}} + B \sqrt{\frac{(B/A)^2}{1 + (B/A)^2}} - \frac{Mo}{K}$$

Realizing that $A = \frac{Mo}{K}$, and collecting terms,

$$\theta max = A \sqrt{1 + (B/A)^2} - A$$

$$\left(\frac{\theta max}{A} + 1 \right)^2 = 1 + (B/A)^2$$

$$B^2 = \theta max^2 + 2 A \, \theta max.$$

Taking the square root and substituting for B and A,

$$i = \frac{\sqrt{2KI}}{\ell} \quad \theta max \quad \sqrt{1 + \frac{2Mo}{K \, \theta max}} \quad .$$

But $Mo = K \, \theta p \longleftrightarrow$ where $\longleftrightarrow \theta p$ = preload angle. Thus

$$i = \frac{\sqrt{2KI}}{\ell} \quad \theta max \quad \sqrt{1 + \frac{2\theta p}{\theta max}} \quad .$$

54